PLANNING OF PEVS PARKING LOTS IN CONJUNCTION WITH RENEWABLE ENERGY RESOURCES AND BATTERY ENERGY STORAGE SYSTEMS

SARAH MAHMOUD ATEF HOSNY KANDIL

A THESIS SUBMITTED TO THE FACULTY OF GRADUATE STUDIES
IN PARTIAL FULFILLMENT OF THE REQUIREMENTS FOR THE DEGREE OF
MASTERS OF APPLIED SCIENCE

GRADUATE PROGRAMME IN COMPUTER SCIENCE AND ENGINEERING
YORK UNIVERSITY
TORONTO, ONTARIO

NOVEMBER 2015

Abstract

The last few decades have seen growing concerns about climate change caused by global warming, which is cause primarily by CO_2 emissions. Thus, the reduction of these emissions has become critically important. One of the effective methods for achieving this goal is to shift towards green electricity energy resources and green vehicles in transportation. For these reasons, the goal of the work presented in this thesis was to address the challenges associated with the planning of plug-in electric vehicles (PEVs) parking lots in combination with renewable energy sources (RES) and battery energy storage systems (BESS) in power distribution networks.

This thesis introduces a new planning technique that aims to minimize the overall capital and operational costs, taking into consideration the operational aspects of distribution networks, such as 1) coordinated PEV charging, 2) smart inverter control of renewable distributed generation (DG) units, and 3) smart scheduling of BESS. Moreover, a new model for the PEV coordinated charging demand is introduced in this work. Due to the complexity of the proposed planning approach, a combination between metaheuristic technique and deterministic optimization techniques have been utilized to manage both the planning and operational aspects respectively.

Acknowledgements

All praise is due to Allah almighty, who is the source of all knowledge in this world and whose countless bounties have enabled me to complete this thesis successfully.

I would not have been able to finish my dissertation without the guidance of my committee members, help from friends, and support from my husband and family.

I would like to express my deepest gratitude to my advisor, Dr. Hany Farag, for his guidance, care, and patience and for providing me with such a wonderful atmosphere for conducting research.

I also offer my gratitude to my father and my mother. My research would not have been possible without their help, their constant support and encouragement, and their never-failing good wishes.

Finally, I would like to thank my husband Mostafa, my son Omar, and my daughter Maryam for always standing by me through both the good times and the bad.

Table of Contents

List of Tables

List of Figures

Nomenclature

A. Acronyms

AER	All electric range
BESS	Battery energy storage system
CAES	Compressed air energy storage
cdf	Cumulative distribution function
DG	Distributed generation
DNO	Distribution network operator
ESS	Energy storage system
EV	Electric vehicle
FIT	Feed-in-tariff
IEA	International energy agency
GA	Genetic algorithm
GAMS	General algebraic modeling system
LA	Lead acid
MCS	Monte Carlo Simulation
MINLP	Mixed integer nonlinear programming
MPPT	Maximum power point tracking
PCC	Power conditioning circuit
pdf	Probability density function
PEV	Plug-in electric vehicle
PV	Photovoltaic
RES	Renewable energy source
RTS	Reliability test system
SMES	Superconducting magnetic energy storage

SOC	State of charge

B. Functions

$CDF^{-1}_{A(d,h)}$	The inverse of the cdf describing the arrival rates
$CDF^{-1}_{T(d,h)}$	The inverse of the cdf of the parking duration
$f^{CH}_{(i,d,h,s,v)}$	The relation between P^{max}_{CH} and the SOC level

C. Indices

d	Index of days
h	Index of time or hours
i, j	Indices of load points
s	Index of scenarios
v	Index of vehicles

D. Parameters

$Eff_{BAT(i)}$	The BESS efficiency
pf_{PV}	Minimum power factor of the smart PV inverter
$A_{(d,h,s)}$	The arrival rates in vehicle/h
$C_{BES_{OM}}$, $C_{BES/kWh}$	The operational and maintenance cost and the BESS capital cost per kwh
$C_{EV\_CH}, N_{EV\_CH(i)}$	Cost and number of installed PEV chargers
$C_{PV/kW}, C_{BES/kW}$	The capital cost of PV panels and BESS in $/kw
C_{kWh}	The price of energy in $/kwh
$E_{BAT-MAX(i)}$	The rated kwh of the BESS

$E_{REQ(i,d,s,v)}$	The required kwh by vehicle v
$I_{MAX(i,j,d)}$	The capacity of the line between buses i, j in day d
LT, LV	Life time of equipment and the levelized cost factor
$N_{VH(h)}$	The total number of vehicles that arrive for hour h
N_{WD}, N_{WE}, N_{yr}	Number of weekdays, weekends, and total number of days in each season
N_s	Number of virtual scenarios
$\mathbb{P}_{(s)}$	The probability of occurrence of scenario s
$P_{CH}, P_{CH}^{max}, P_{CH}^{capcity}$	The allowable, maximum PEV manufacturer, and maximum charger rates respectively
P_{MAX}^{Rev}	The allowable maximum reverse active power
P_{total}	Number of pdfs to be tested
$Q_{BAT-MAX(i,h,d,s)}$	The maximum allowed BESS reactive power
r, f	Interest and inflation rates
$SOC_{BAT-MIN(i)}$	The minimum allowed SOC of the BESS
$T_{(d,h,v)}*$	The parking duration in hours for vehicle v
$U_{(s)}$	A uniformly distributed random number from 0 to 1
V_{min}, V_{max}	The minimum and maximum voltage limits
$Y_{(i,j)}, \theta_{(i,j)}$	Magnitude and angle of Y-bus entry
η_{CH}	The charger efficiency

E. Sets

$\mathcal{I}_{BES}$	Set of candidate system buses for BESS installation
$\mathcal{I}_{EV}$	Set of candidate system buses for PEV stations
$\mathcal{I}_{PV}$	Set of candidate system buses for PV DG installation

F. Variables

$a_{BES(i)}$, $a_{PV(i)}$	Binary variable indicating the decision of installing BES and PV DG respectively
$\mathscr{b}_{BES1(i)}$ $\mathscr{b}_{BES2(i)}$	Integer variable indicating the size of BES kw and kwh respectively
$\mathscr{b}_{EV(i)}$	Integer variable indicating the number of charging stations installed at bus i
$\mathscr{b}_{PV(i)}$	Integer variable indicating the size of PV DG
$C_{Loss(s)}, C_{cons(s)}$	The costs of energy losses and energy consumed by BES, PEVs, and normal load
C_{PV}, C_{BES}, C_{EV}	The capital and operating costs for the PV DG, BES, and PEV chargers respectively
$E_{BAT(i,d,h,s)}$	The stored energy in the BESS
$E_{D(i,d,s,v)}$	The delivered kwh to vehicle v
$G_{PV(s)}, G_{PV/kWh}$	The profit of selling energy from solar based DG and the price of per kwh
$I_{(i,j,h,d,s)}$	The current between buses i, j
$P_{BAT-MAX(i,d,h,s)}$	The maximum allowable BESS active power transfer
$P_{BES_{kW}}, P_{BES\_kWh}$	Installed kW and kWh capacity of BESS
P_G, Q_G	The active and reactive generated powers
P_{loss}	The active power loss
P_L, Q_L	The active and reactive consumed powers
P_{g-BAT} , Q_{g-BAT}	Is the generated active and reactive powers from BESS
P_{PV_CAP} , P_{PV}	Installed capacity and generated active power form solar based DG
P_{NL}, P_{PEV}	Consumed active power by normal load and PEVs
$Q_{PV(i,h,d,s)}$	Reactive generated power from PV DG
$SOC_{(i,d,h,s,v)}$	The PEV battery SOC in %

$V_{(i,d,h,s)}, \delta_{(i,h,d,s)}$	Magnitude and angle of voltage
X_{P-BAT}, X_{Q-BAT}	The decision of injecting or absorbing active and reactive powers for BESS
X_{P-PV}, X_{Q-PV}	The decision of curtailing the active and reactive generated powers from PV DG respectively,
$X_{EV(i,d,h,s,v)}$	The decision of charging PEV v
Ω_1	The vector of decision variables for capacity planning
Ω_2	The vector of decision variables for PEV and DER operational schedule

Chapter 1
Introduction and Motivations

Reducing greenhouse gas emissions have gained global interest over the last few decades. A key factor for reducing these emissions is shifting towards RES in electricity generation and low or zero-emission vehicles in transportation. Electrification of the transportation sector is currently the most viable option for reducing transportation emissions and the deployment of PEVs is thus predicted to rise dramatically in the next few decades [1]. Some countries put targets up to 7.9 M electric vehicles by 2030 [2], as reported by IEA (see Table 1-1).

Current power grid structure is capable of accommodating low penetration levels of uncontrolled PEV charging (i.e. charging starts as soon as PEVs are plugged). However, looking to the future, the increasing use of PEVs will have a considerable impact on the demand for electricity and the development of future power grids. Recent studies showed that the rapid growth of PEVs along with the additional energy consumption likely to cause severe consequences on the existing grids [3-6]. Hence, accommodating the extra load on the grid due to PEV charging will require: 1) upgrading the existing power distribution system infrastructure so that it can accommodate uncoordinated charging, and/or 2) integration of smart grid technologies to coordinate PEV charging via real-time monitoring and control (i.e. optimally scheduling of PEVs charging, where the battery pack of PEV acts as a controllable load) [7, 8].

Table 1-1: Announced national PEV targets [2]

Country	Target [2]
Ireland	2020: 230 000
Canada	2018: 500 000
United States	2015: 1 000 000
France	2020: 2 000 000
Spain	2020: 2 500 000
United Kingdom	2030: 7 900 000

Yet, supplying the extra load imposed by charging PEVs from conventional electricity generation resources will shift the emissions from the transportation to the electricity generation. To allay this concern, RES are expected to play an important role in supplying energy to the transportation sector [9, 10]. Levels of RES deployment have been rising satisfactorily due to government incentives and developing technology in this area [11, 12]. However, integrating large levels of renewable distributed generation (DG) into the grid is also challenging as the variable and unpredictable nature of wind and solar exposes the grid to stability issues and makes the investment planning of future power grids more complicated [13]. Despite these challenges, other considerations show promise. Storage systems (e.g. BESS) can be a critical component of grid stability and resiliency [14]. The grid integration of energy storage technologies would reduce the intermittency of RES, thus increasing their capacity factor [15]. Storage systems can also prevent wastage of excess renewable energy feeding into the grid at times when production is at a peak, but demand is low by effectively storing this energy [16]. In

addition, integrating BESS into existing grids could enable confident deployment of PEVs by ensuring a stable and consistent supply of the electricity vital to charge their batteries [17].

The combined integration and advancement of PEVs, RES, and BESS technologies has been recently gained interest in industry [18, 19]. This in turn introduces paradigm shift in distribution systems operation and planning. Due to the interesting and recent subject, numerous efforts have been spent on related research. Yet, most of the work in this area focused on optimal PEV coordination in real-time, without considering the planning aspects (i.e. the location and sizing of PEV charging stations along with RES and BESS), which has significant impacts on 1) the overall system performance, and 2) the effectiveness of the real-time coordination schemes.

It is expected that PEVs will likely be concentrated in specific geographical areas, which if not properly managed, may have severe consequences on the electrical grid, such as feeders' thermal limit violation, phase imbalance, transformer degradation, and fuse blowouts [20]. Planning the location and sizes of PEV parking lots in electrical distribution systems thus requires further study and analysis.

Optimal allocation and sizing of such new technologies should be appropriately integrated in distribution networks investment planning studies in order to: 1) get the highest benefit from the environmental aspects, 2) bring economic benefits for the system operators and their stakeholders and, 3) enhance the system reliability, stability and resiliency.

Therefore, the work presented in this thesis proposes a new comprehensive framework for the planning studies of smart distribution systems including PEVs.

Conventional planning studies are not tailored for accommodating new smart distribution systems planning studies, given that they rely on dedicated distribution systems with conventional loads, deterministic distributed generation units, and lack of two-way communications, which is anticipated to be the backbone of the smart grid.

Therefore, the proposed framework integrates the key components of smart distribution system: renewable distributed generation, battery storage system, electrical vehicles, and two-way communication system.

The proposed planning approach considers smart coordinated charging system, which utilizes real-time measurements from the electrical smart grid and coordinates the PEV charging under the smart grid paradigm.

1.1 Research Objectives

The aim of this research is to develop a comprehensive planning framework to allocate PEV parking lots in conjunction with RES and BESS taking into consideration different operational aspects. Toward this aim, the work presented in this thesis is divided into three main objectives, as depicted in Figure 1-1. A brief description of each objective is presented below in the following subsections.

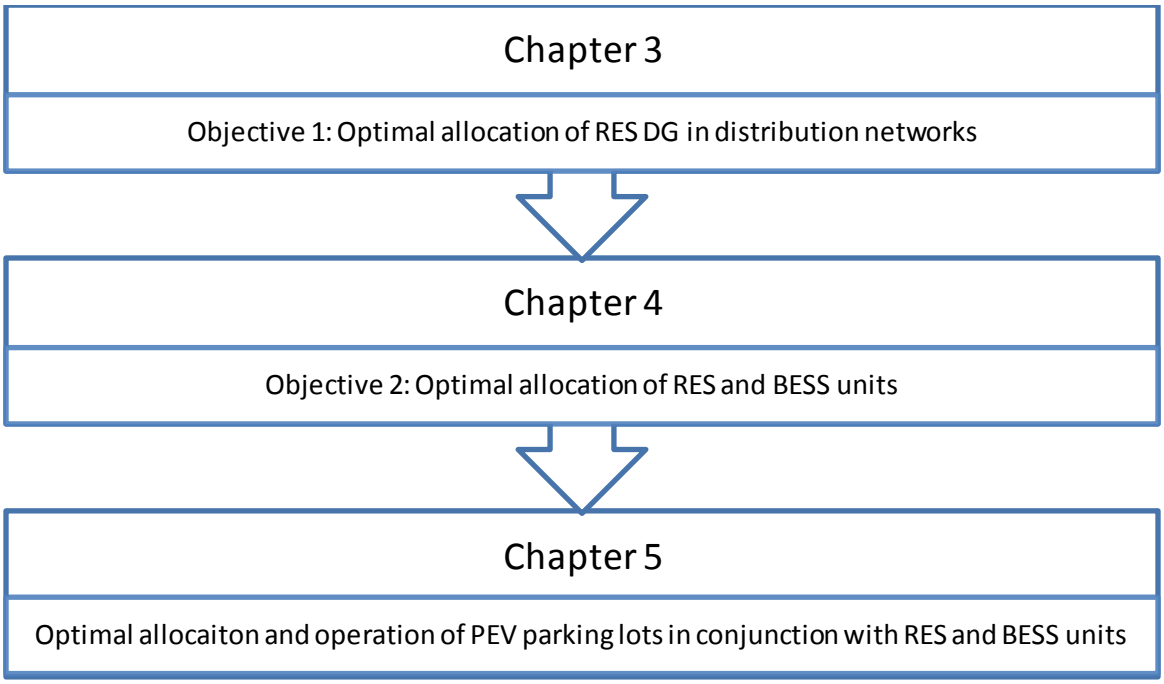

Figure 1-1: Research objectives

1.1.1 Objective (1): Optimal allocation of RES DG

The goal of the first objective is to develop a planning approach for the optimal location and sizes of renewable DG units taking into consideration: 1) the uncertainty due to the intermittent nature of RES output power, and 2) the variability of conventional power loads. Toward this objective, probabilistic models for both RES and loads are developed and incorporated in the optimization problem. The developed optimization approach has been utilized to investigate the impacts of the distribution network technical constraints on the allocation process, to identify the most significant binding constraints.

1.1.2 Objective (2): Optimal allocation and operation of RES and BESS

In the second objective, the task is to develop methodologies for optimal allocation of renewable DG in conjunction with BESS units in distribution networks taking in to consideration the operational aspects of these units. The operational aspects include: 1) controlling the smart inverter of the renewable DG units, and 2) optimal scheduling of BESS units to achieve minimum overall system costs. To that end, Monte Carlo Simulation has been used to develop virtual chronological scenarios of RES output power.

1.1.3 Objective (3): Optimal allocation and operation of PEV parking lots

The third objective aims to develop a comprehensive planning framework to allocate and size PEV parking lots in distribution networks. Smart coordination of the PEV charging is considered as the operating scheme of these PEV parking lots. Moreover, as a mean to facilitate the allocation, RES and BESS allocations are considered in the same planning approach. The RES and BESS should be optimally sized and scheduled to serve the PEV charging requirements. A new model is introduced to incorporate the smart PEV parking lots into the planning approach.

1.2 Thesis outline

The remainder of the thesis is organized as shown above in Figure 1-1. The details of each chapter are as follows:

- Chapter 2 provides a brief review of the background topics and associated literature pertinent to this research.
- Chapter 3 presents the proposed approach for the optimal allocation of renewable DG along with related simulation results.
- Chapter 4 describes the proposed planning approach for the renewable DG and BESS optimal allocation and operation.
- Chapter 5 introduces the proposed planning method for PEV parking lots in conjunction with RES and BESS along with related models.
- Chapter 6 concludes the research and offers suggestions for future work.

Chapter 2
Background and literature review

Chapter 1 provided a brief introduction to the research presented in this thesis, explaining the motivation behind the work and outlining the specific objectives. This chapter provides an introduction to the new components of smart distribution networks (i.e., RES, BESS, and PEV) and their modelling in the planning problem of future distribution networks. The introduction is followed by a discussion of previous research. Finally, the concluding remarks from previous research are highlighted.

2.1 Background to RES

Renewable energy is generated from sustainable resources that are naturally renewed within human life [21]. These resources include but not limited to flowing water, moving air, solar radiation, and geothermal. Other resources can be assumed renewable, such as biomass, as long as the rate of its consumption is lower than the rate of its production.

Canada is a world leader in renewable energy resources. Ontario province has 34,780 MW of installed generation with a supply mix as shown in Figure 2-1 as of June 2015 [22]. RES presents about 34 % of the total installed capacity.

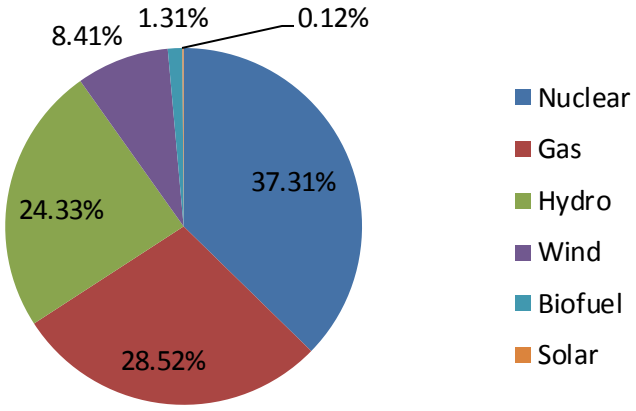

Figure 2-1: Ontario supply mix as of June 2015 [22]

Hydroelectricity has the biggest share of the renewable energy production in Ontario, as shown in Figure 2-1. However, wind and solar RES are expected to have the highest growth rate in the next few years [21].

A brief overview of the available RES technologies can be explained as follows [23]:

2.1.1 Hydroelectricity

Electricity is generated through transforming the useful kinetic energy offered by moving water into electrical energy. Mainly, the moving water is directed to the rotating turbine blades; thus, producing a rotating mechanical energy. These turbines are in turn connected to electricity generators, which converts the mechanical energy into electric energy and supply it to the electric grid.

Dams and gates are used to regulate the water volume and speed, which in turn regulates the amount of electricity generated. Hydroelectricity generation stations are highly

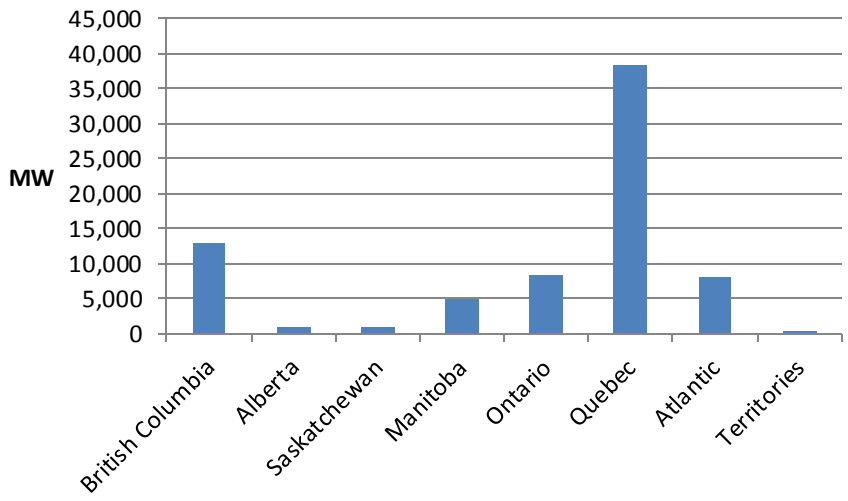

Figure 2-2: Installed Hydroelectric Capacity by Provinces (2010, in megawatts) [21]

dependent on the geography and hydrography [21]. This is the reason for the province of Quebec to have the highest installed hydro capacity in Canada [21], as shown in Figure 2-2.

Canada has many rivers flowing from mountainous areas toward its three bordering oceans. In 2010, Canada had 529 hydroelectric stations with more than 75 thousand megawatts of installed capacity. These stations include 379 small hydroelectric facilities, that is, facilities with a nameplate capacity of 50 megawatts or less, and they together represent 3.5 thousand megawatts, which is about 2.7% of Canada's installed capacity. A study by HEC Montréal (formerly known as: École des hautes études commerciales de Montréal) shows that by 2030, there is a potential in Canada for new hydroelectricity capacity installed of 29,000 MW [21].

2.1.2 Bioenergy

This RES relies on biological materials (solid, liquid, or gaseous) as a fuel, where the chemical stored energy is converted to electricity. The biomass fuel is combusted to produce heat, which can be used directly in industrial processes or to heat up steam, which is used to rotate a turbine and a generator to produce electricity. Industrial wood waste is the most important source of bioenergy in Canada [21].

2.1.3 Geothermal Energy

Geothermal energy is generated by earth stored heat. The geothermal energy can be harvested from natural underground steam, which in turn is used to generate electricity. Another approach is to use the temperature difference between ambient air temperature and the ground water for heating or cooling of buildings in order to save electricity.

The highest potentials for geothermal energy harvesting are in British Columbia, Northwest Territories, Yukon, and Alberta, where highest underground temperatures are available. The most advanced geothermal power generation project in Canada is the South Meager project in British Columbia [21].

2.1.4 Wind Energy

Kinetic energy in wind is one of the most promising RES. It can be easily used to rotate wind turbines, which in turns produce electricity. For thousands of years the kinetic energy in wind has been used for propelling sailing ships, pumping water, and powering factory machinery [23].

The first wind turbine to produce electricity was built in 1891 by a Dane, Poul la Cour. Currently, many wind farms are located in high wind areas to produce efficient electric energy over the year. The wind turbines are characterized by long life time and low maintenance requirements. Wind turbines range from few kW and up to 8 MW (Vestas V164-8.0).

There are excellent wind resource areas in Canada, which are mainly offshore and along coastlines [21]. Wind turbines installed capacity in Canada has increased rapidly in the recent years. Canada has 10,204 MW installed capacity in 2015 compared to 5,265 MW in 2011 and 23 MW in 1997. The provincial leaders in installed wind turbines capacity are Ontario, and Quebec, as shown in Figure 2-3.

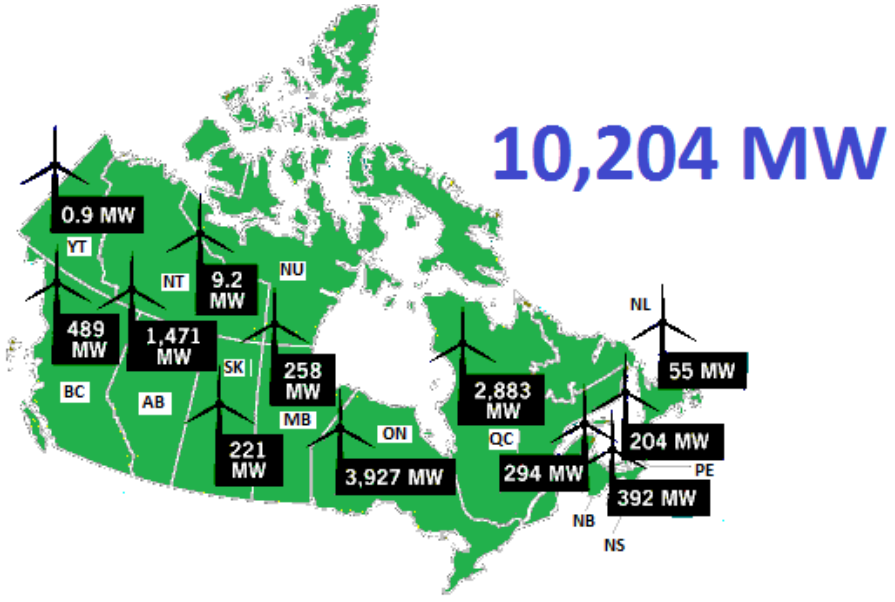

Figure 2-3: Canada's installed wind turbines capacity as of June 2015 [24]

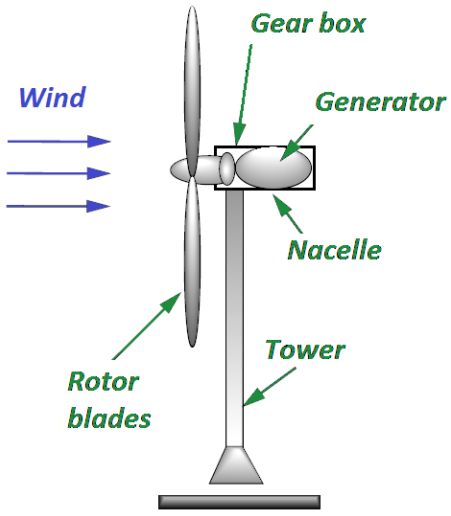

Figure 2-4: Horizontal axis wind turbines structure [23]

The most popular wind turbine structure is the horizontal axis wind turbines. These wind turbines mainly consist of blades, generator, gear box, and tower as shown in Figure 2-4.

2.1.4.1 Wind Power

The wind energy that can be harvested depends on the sweep area of the turbine blades and the wind speed [23], as in (2-1). It is noteworthy that the wind output power is proportional to the square of the blades diameter as $A_s = \left(\frac{\pi}{4}\right) D^2$. Thus, doubling the diameter of the blades increases the power by four times. Moreover, the power is proportional to the cube of the wind speed, which means doubling the wind speed increases the power by eight times.

$$P_w = \frac{1}{2}\,\rho\, A_s v_w^3 \qquad \textbf{(2-1)}$$

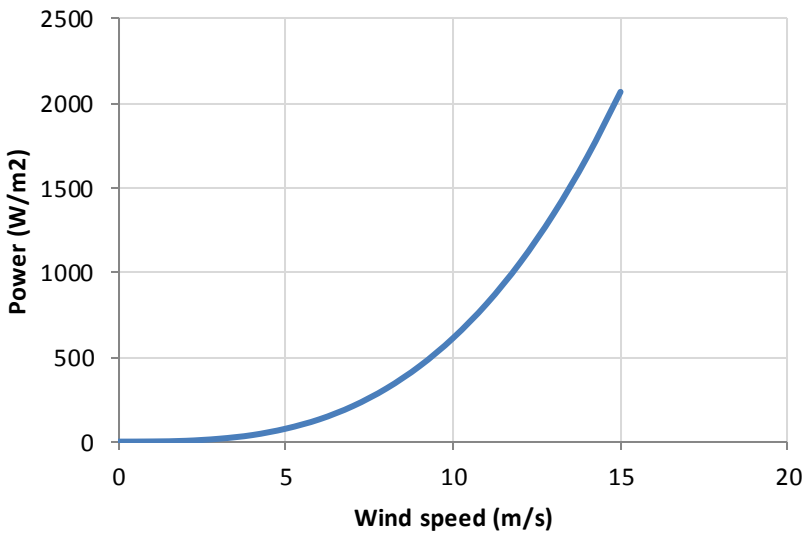

Figure 2-5: Wind power per unit area for 15°C and 1 atm [23]

A typical wind power relation versus wind speed per unit sweep area is shown in Figure 2-5.

2.1.4.2 Impact of tower height

Due to the fact that wind power is proportional to the cube of the wind speed, the height of the wind turbine is very important economic aspect in the wind turbine design and harvesting energy. As the tower height increases, the wind speed increases [23]. However, this depends on the friction that the air experiences when it moves across the earth's surface. The smoother the surface, the faster the wind speeds can be at higher heights. The impact of the surface roughness can be expressed by the following formula [25]:

$$v_2 = v_1.\left(\frac{\ln(\frac{h_2}{z_0})}{\ln(\frac{h_1}{z_0})}\right) \quad \textbf{(2-2)}$$

The roughness factor (z_0), which varies from 0.0002 to 1 [26], for different terrain descriptions is listed in Table 2-1.

Table 2-1: Roughness factor for different terrains [26]

Terrain Description	z_0 (m)
Open sea, fetch at least 5 km	0.0002
Mud flats, snow; no vegetation, no obstacles	0.005
Open flat terrain; grass, few isolated obstacles	0.03
Low crops, occasional large obstacles	0.10
High crops, scattered obstacles	0.25
Parkland, bushes, numerous obstacles	0.50
Normal large obstacle coverage (suburb, forest)	1.0
City centre with high- and low-rise buildings	≥ 2.0

2.1.4.3 Wind turbine output power

The wind turbine output power characteristics as given in a manufacturer data sheet depend on four parameters: rated output power, cut-in speed, rated speed, and cut-out speed, as in (2-3). These characteristics are also illustrated in Figure 2-6.

$$P_{WT}(v) = \begin{cases} 0 & \forall\ 0 \le v < v_{in} \\ P_{WT}^{rated}.\left(\frac{v - v_{in}}{v_{rated} - v_{in}}\right) & \forall\ v_{in} \le v < v_{rated} \\ P_{WT}^{rated} & \forall\ v_{rated} \le v < v_{out} \\ 0 & \forall\ v_{out} \le v \end{cases} \quad \textbf{(2-3)}$$

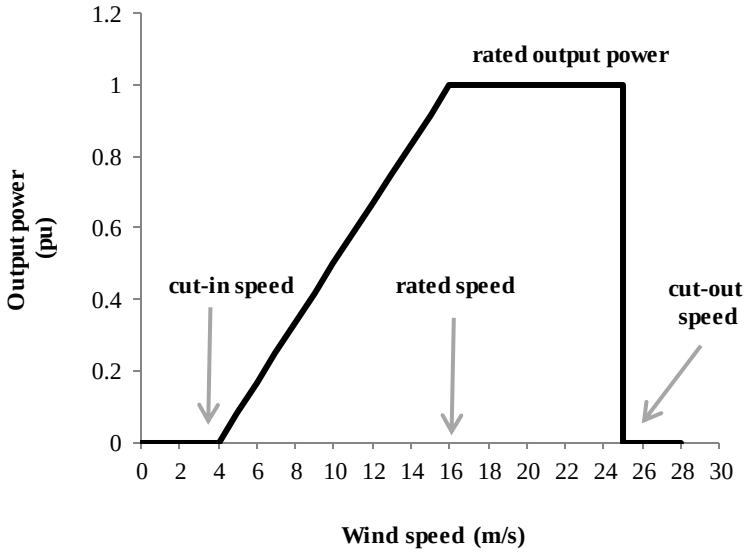

Figure 2-6: Wind turbine output power [27]

2.1.4.4 Wind DG modeling for planning applications

Due to the fact that RES are characterized by a high degree of uncertainty and variability, probabilistic methods are used to model these types of resources for the planning applications. On the other hand, for few minutes and up to few days operational applications, these resources can be forecasted using proper forecast methods.

For wind turbines, Weibull Probability density function (pdf) $f_{WB}(v)$ is considered as the most commonly used pdf to represent the wind speed variability [28], and in consequence the wind turbines output power. The Weibull pdf formula [29] given in (2-4) defines the probability of wind speed to be equal to or less than a specific speed v.

$$f_{WB}(v) = \frac{k}{c}\left(\frac{v}{c}\right)^{k-1} exp\left(-\left(\frac{v}{c}\right)^{k}\right) \quad \textbf{(2-4)}$$

The formula in (2-4) depends on two parameters to fit the pdf to the historical measured wind speeds. These parameters can be calculated using the average wind speeds and the standard deviation of the historical wind speed data [29], as in (2-5) to (2-8).

$$k = \left(\frac{\sigma}{\bar{v}}\right)^{-1.086} \quad \textbf{(2-5)}$$

$$c = \frac{\bar{v}}{\Gamma(1 + \frac{1}{k})} \quad \textbf{(2-6)}$$

$$\bar{v} = \frac{\sum_{u=1}^{N} v_{(u)}}{N} \quad \textbf{(2-7)}$$

$$\sigma = \sqrt{\frac{\sum_{u=1}^{N} (\bar{v} - v_{(u)})^2}{N - 1}} \quad \textbf{(2-8)}$$

2.1.5 Solar Energy

Solar energy is available as radiated heat and light from the sun. Solar energy can only be collected during the day light and are affected by clouds or other obstacles.

Nowadays, two main technologies are used to convert the solar energy to usable energy [23]:

- Solar collectors, which are used to heat water or air to be used in buildings.
- Solar photovoltaic (PV) cells which converts solar irradiation directly to electricity.

Recently, Canada installed capacity of solar energy has increased, although it is still relatively small compared to the size of the energy market (0.12 % of the total installed

electricity generation capacity, as shown in Figure 2-7) However, with the reduction of the photovoltaic system prices, which has been reduced to one third in the last six years [30], the installed capacity of photovoltaic systems is expected to increase rapidly. This is also due to the incentives given by the Canadians government for RES installation, especially photovoltaic systems, which can sell their generated energy to the grid with up to 38.4 ¢/kWh, as shown in Table 2-2. Moreover, Canada south regions have a great potential for solar energy generation, as shown in Figure 2-7.

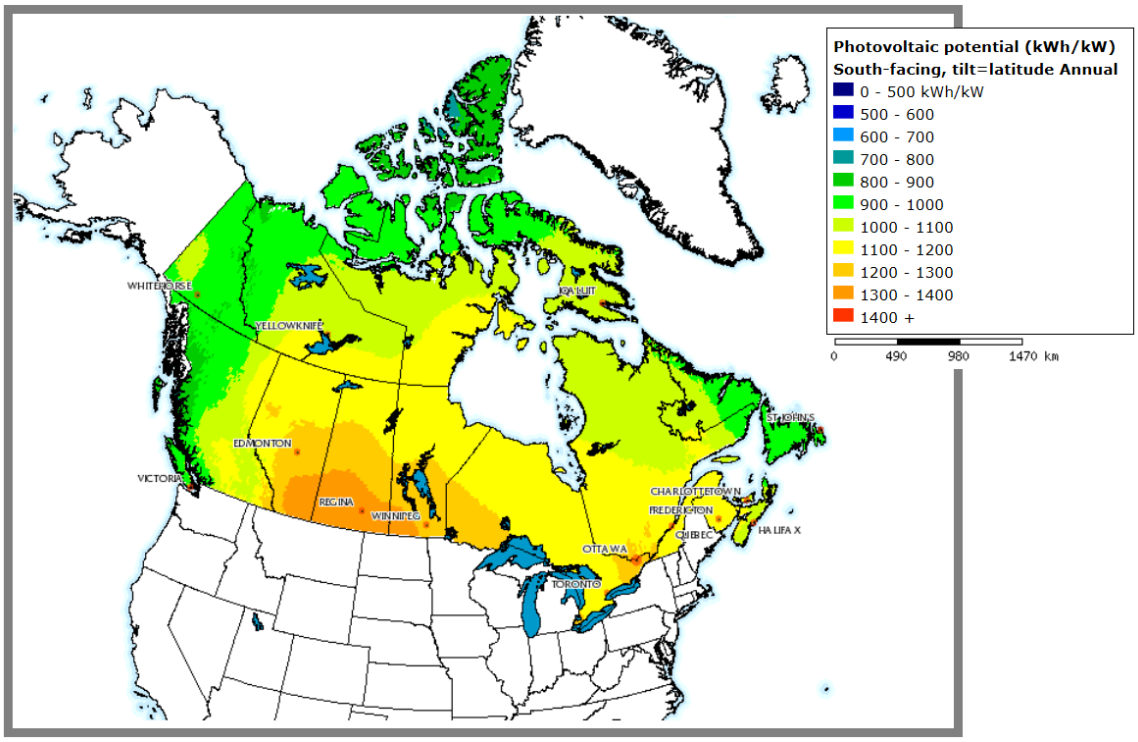

Figure 2-7: Annual Photovoltaic potential and solar resource maps of Canada [21]

Table 2-2: FIT/microFIT price schedule [31]

Renewable Fuel	Project Size	Price (¢/kWh)
Solar (PV) (Rooftop)	≤ 10 kW	38.4
	> 10 kW ≤ 100 kW	34.3
	> 100 kW ≤ 500 kW	31.6
Solar (PV) (Non-Rooftop)	≤ 10 kW	28.9
	> 10 kW ≤ 500 kW	27.5

The photovoltaic potential is the amount of electricity in kWh that can be generated annually on the average lifetime of the typical photovoltaic system per kW installed capacity. The potential of solar energy is lower in coastal areas in Canada and is higher in the central areas. Despite this, installing solar panels on residential buildings roofs can meet about half the residential electricity demand in Canada [21].

Most of these RES are geographically dependent. However, solar energy is one of the most promising source of energy due to the fact that it can be implemented anywhere on earth. They have wide variety of sizes that range with few watts and up to MW. The solar panels can be placed on ground, or can be roof top.

Besides solar panels, wind turbines currently are offered in the market with wide range of capacities that ranges from few kW and up to few MW for a single unit. Smaller units are available in roof mount structure.

2.1.5.1 Photovoltaic system structure

An individual photovoltaic cell produces about 0.5 V. These cells are connected in series to form a module with higher voltage, e.g. 12-V module. Further, the modules are connected in series to increase the voltage and in parallel to increase their current. Thus, several modules can be connected in series and parallel to form the photovoltaic array with desired output voltage, current, and power, as shown in Figure 2-8. Further, the photovoltaic arrays are connected to DC/DC converter to boost their voltage and DC/AC converter to interface with the AC grid.

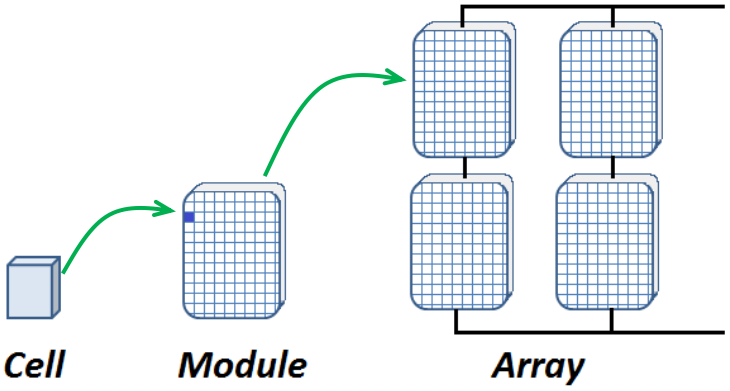

Figure 2-8: Photovoltaic array structure [23]

2.1.5.2 Photovoltaic system characteristics

The photovoltaic array has unique I-V characteristics, depending on the types of cells, and the connection of the cells and modules. Typical I-V characteristics of a PV array are shown in Figure 2-9 at specific solar irradiance and ambient temperature conditions. Three distinct operating points on the PV system characteristics can be identified:

- Short circuit current: this is the current that is delivered by the PV array at a zero terminal voltage, i.e. short circuit.
- Open circuit voltage: this is the voltage generated at the terminals of the PV array when the terminal current is zero, i.e. open circuit.

Maximum output power: this operating point lies near the knee of the I-V curve, where maximum power can be generated from the PV array at the same solar irradiance and ambient temperature conditions. This point is the most desirable operating point; therefore, maximum power point tracking (MPPT) techniques are used to track this point at any solar irradiance and ambient temperature.

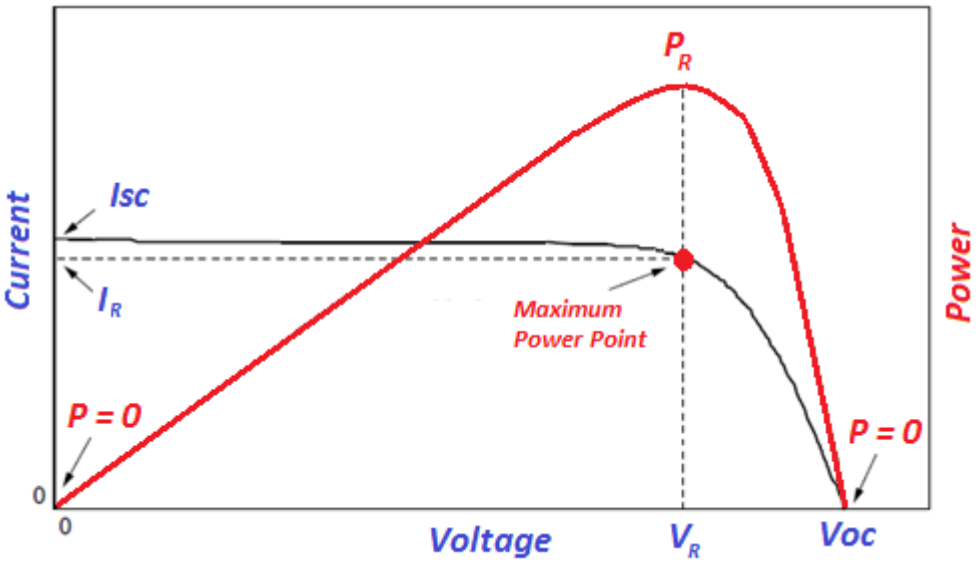

Figure 2-9: The I-V characteristics of a typical PV array [23]

2.1.5.3 PV system output power

As mentioned before, the output power of the PV system depends on the PV modules characteristics, solar irradiance, and ambient temperature. The output power of a PV module assuming MPPT can be calculated using [28]:

$$T_{cell} = T_A + S_{IR} \times \left(\frac{T_{nom} - 20}{0.8}\right) \quad \textbf{(2-9)}$$

$$I_{PV} = S_{IR} \times (I_{sc} + K_i(T_{cell} - 25)) \quad \textbf{(2-10)}$$

$$V_{PV} = V_{OC} - K_v T_{cell} \quad \textbf{(2-11)}$$

$$P_{PV} = N_{cells} \times FF \times V_{PV} \times I_{PV} \quad \textbf{(2-12)}$$

$$FF = \frac{V_{MPP} \times I_{MPP}}{V_{OC} \times I_{SC}} \quad \textbf{(2-13)}$$

2.1.5.4 PV DG modeling for planning applications

Due to the intermittent nature of the PV panels output power, a probabilistic model is used to model these types of RES [28]. For a specific hour during the day, the solar irradiance is usually modeled with a Beta pdf, which best describes the solar irradiance behaviour. The Beta pdf can be given as [28]:

$$F_{Beta}(S_{IRR}) = \begin{cases} \frac{\Gamma(\alpha+\beta)}{\Gamma(\alpha)\Gamma(\beta)} S_{IRR}^{(\alpha-1)} (1 - S_{IRR})^{(\beta-1)} & \forall\, 0 \le S_{IRR} \le 1, \alpha \ge 0, \beta \ge 0 \\ 0 & otherwise \end{cases} \quad \textbf{(2-14)}$$

$$\beta = (1 - \mu_{IRR}) \times \left(\frac{\mu_{IRR}\ (1 - \mu_{IRR})}{\sigma_{IRR}^2} - 1 \right) \quad \textbf{(2-15)}$$

$$\alpha = \frac{\mu_{IRR}\ \beta}{1 - \mu_{IRR}} \quad \textbf{(2-16)}$$

2.2 Background to battery energy storage systems

Several technologies are available as means of electrical energy storage system (ESS). Any energy storage system consists of two basic components: energy storage reservoir and a power conditioning circuit (PCC) [32]. The function of the PCC is to convert the energy from the grid to a form that can be stored in the storage system, and vice versa. The PCC can be a power electronics converter as in batteries or a motor-generator set as in pumped hydro [32, 33].

The available ESS technologies can be categorized according to their application, which varies from power quality, bridging power, and energy management purposes, which can be briefly explained as follows (also illustrated in Figure 2-10) [32-35]:

- For power quality applications, the energy stored in the ESS is used to enhance the power quality of the power system, such as improving the voltage profile. These applications require responding time in the range of seconds or fraction of seconds. This can be achieved by flywheels, capacitors, and BESS technologies.
- Bridging power applications are used to ensure continuity of the electricity supply whenever switching from one source of power to another occurs. This application requires respond time in the range of seconds and up to minutes. BES and

superconducting magnetic energy storage (SMES) technologies can be used for this purpose.

- Energy management is used to reshape the energy consumption curves by storing energy during off-peak or low prices periods and using this energy during peak or high prices periods. BES, SMES, pumped hydro, and compressed air energy storage (CAES) technologies can be used for this application which has a time span of hours.

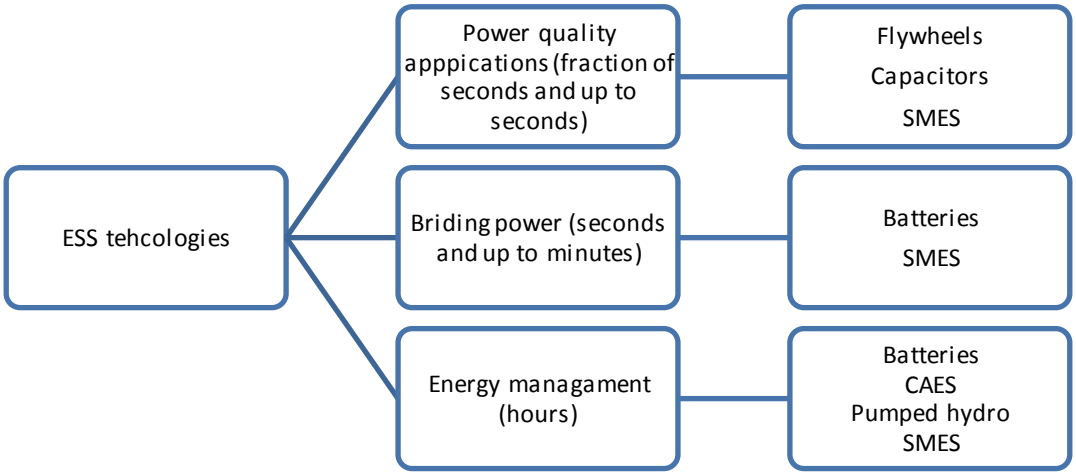

Figure 2-10: ESS technologies classification according to the application [35]

Each ESS technology has unique characteristics, which depends on the medium in which the energy is stored. The physics behind each energy storage technology and the advantages/disadvantages of each technology are described briefly as follows [32, 33, 36-38]:

- SMES stores energy in the form of magnetic field, which is generated by current flowing in a superconducting coil, which is made of special alloy and maintained at very low temperature to reduce its resistance to be almost negligible. Although this technology has high efficiency and long life time, it is very expensive to implement.
- Energy is stored in capacitors in the form of electrical field. Capacitors have high efficiency and long life time; however, they provide only short-term storage. Super capacitors are also available, which can store more energy for longer time periods; however, this technology is expensive compared to other ESS.
- Batteries are the most popular ESS, which store energy in the electrochemical form. BESS has lower life time and lower efficiency (60-80 %) compared to other ESS. Several types of batteries are available based on the material used in manufacturing: LA, Na/S, Ni/Cad, and VR batteries.
- Flywheel stores electrical energy in the form of kinetic energy in a rotating mass. Flywheels have fast response, good efficiency, and long life time; however, they can deliver energy for short time periods.
- CAES stores energy in the form of compressed air. Further, the compressed air is used to produce electrical energy. it has moderate efficiency and life time. This technology is highly dependent on the geography and cannot be economical feasible except in special locations.

- Pumped hydro storage is widely used, where water is pumped to high altitudes and used to drive hydro-turbines and produce electricity when needed. This technology store the electrical energy in the form of potential energy stored in the pumped water. This technology is geography dependent, and requires building dams.

Therefore, each technology has its power ratings and response time, which determine the proper application for each ESS type. Figure 2-11 shows the comparison between different technologies as reported by Electricity Storage Association and shown in [32].

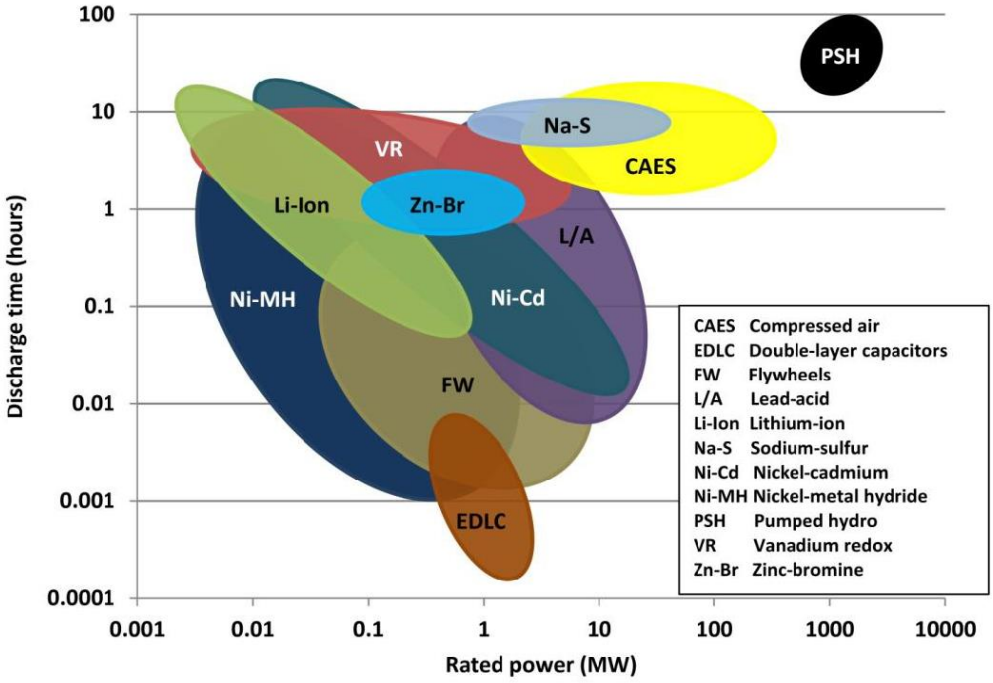

Figure 2-11: Power rating and discharge time for different ESS technologies [32]

A recent project in Canada by Toronto Hydro was installed with rating of 500 kW-250 kWh [39]. Ontario government also put a plan for a total of 50 MW of ESS to be installed by the end of 2016 [40].

ESSs have very expensive capital costs. The installation cost of ESS has been reduced by 50 % in the last decade, and is expected to decrease further to less than $600 /kW by 2020, as shown in Figure 2-12.

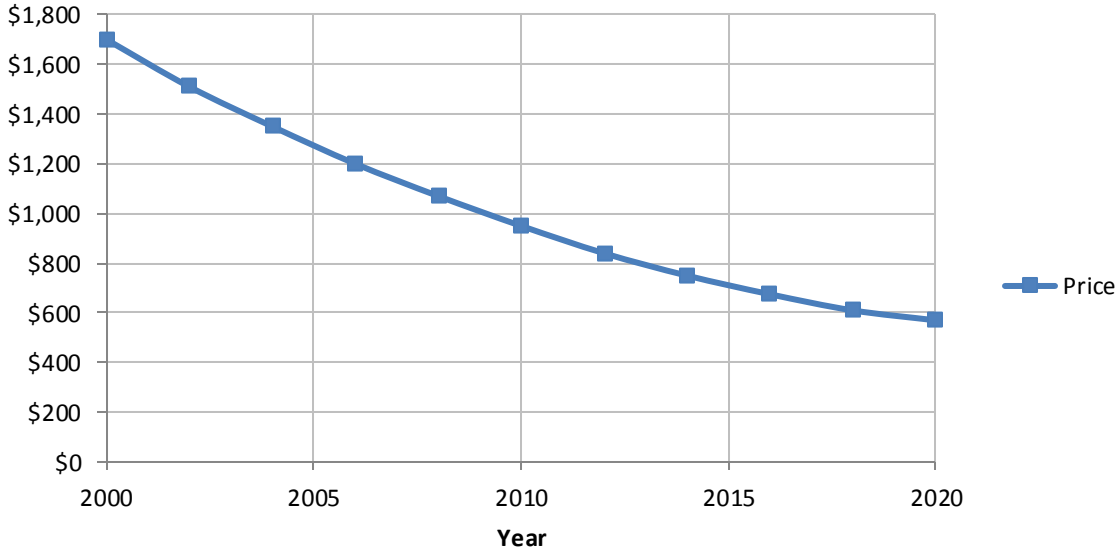

Figure 2-12: Historical and projected installation cost of ESS per kW [41]

2.2.1 BESS modeling for planning applications

The BESS in this work are assumed to be four quadrants, as shown in Figure 2-13. Technical limitations on the stored energy, state of charge (SOC) level, charge/discharge rates, and reactive power limits should be considered in the model. Thus, at any instant of

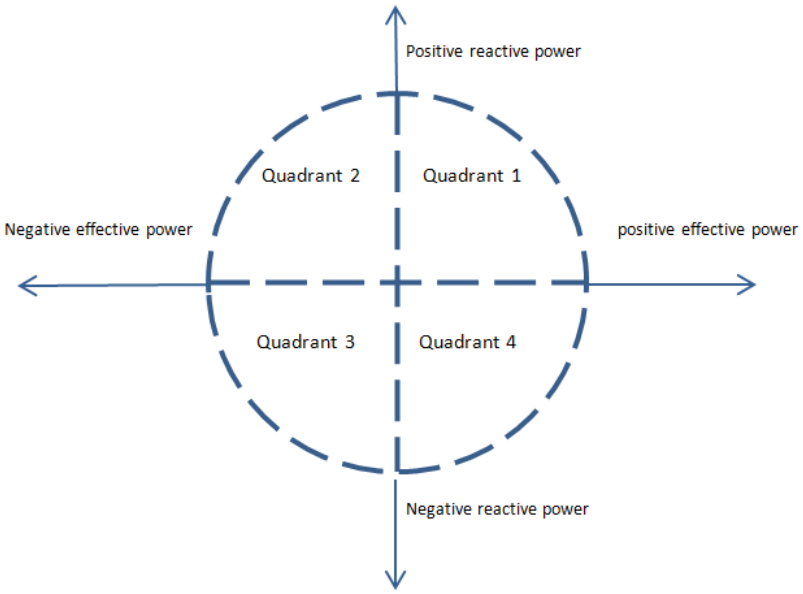

Figure 2-13: Four quadrant BESS characteristics

time, the active and reactive power produced or absorbed by the BESS should not exceed the capability limits given in Figure 2-13, i.e.

$$P^2 + Q^2 \leq S_{MAX}^2 \qquad \textbf{(2-17)}$$

where P and Q are the active and reactive powers produced or absorbed by the BESS and S_{MAX} is the maximum apparent power of the BESS in kVA. The value of S_{MAX} in practical changes is based on the BESS temperature; however, for simplicity, the effect of temperature variation is ignored in this work. Moreover, the SOC at any instant of time shouldn't reach below a minimum value according to the BESS specifications.

2.3 Background to Plug-in Electric vehicles

The electric vehicle (EV) is a vehicle with a driving torque produced by an electric motor. The source of the electric energy to this motor and how this energy is delivered define the type of the EV. Three types are currently available: hybrid electric vehicle (HEV), PEV, and fuel cell EV. A brief description of each type is given hereunder.

- The HEV has a conventional fossil fuel engine, which provides the required electric energy to the driving motor. Although it has better fuel efficiency compared to conventional vehicles, the only source of energy is the fossil fuel.
- The PEV is a vehicle with a higher-capacity battery that can restore its charge from an external electric power source. These vehicles may contain a conventional fossil fuel engine to extend the driving range or it may be pure EV. Some of these vehicles may restore the charge of the battery by swapping their batteries with another charged battery without the need to connect to an external electric power source.
- The third type is the fuel cell EV. These vehicles are equipped with fuel cell technology which converts chemical energy stored in fuel (usually hydrogen) to electric energy, which is supplied to the motor. These vehicles are more expensive compared to PEV. Moreover, hydrogen fueling stations infrastructure requires massive investments. On the other hand, the electric power system is almost available everywhere.

PEV is the most popular type of EVs, due to its low running cost and the availability of charging outlets. However, still the capital cost of the battery pack system is a challenge.

The sizes of the batteries of these vehicles are determined by the vehicles class (sedan, SUV, pick-up, …, etc.) and all electric range (AER) [3]. The AER is the total distance that the vehicle can be driven in pure electric mode, i.e. battery depletion mode. In this mode, the stored energy in the battery is used to power the electric motor [3]. On the other hand, when the PEV is equipped with a fossil fuel engine, it can be driven in battery sustained mode, where the fossil fuel engine is used to power the electric motor or the engine can be used directly to produce the driving torque [42].

Several types of chargers are available to charge the PEV battery pack from an electric outlet ranging from 3.3 kW (can deliver 3.3 kWh in one hour to the PEV battery pack) and up to 100 kW. However, the most common charger is the 7 kW charger, which is also known as level two charger [43].

A typical PEV charger structure is shown in Figure 2-14. This charger performs two main tasks [44]:

- Converts the AC voltage from the grid to DC voltage via AC/DC power electronics converter.
- Controls the battery pack voltage and current via DC/DC converter.

For a Li-ion battery, usually it is charged in constant-current mode via the DC/DC converter till it reach a high SOC, then the constant-voltage charging mode is used to

avoid overcharging the battery pack, which may destroy it. Typical charging characteristics of a Li-ion battery pack are shown in Figure 2-15.

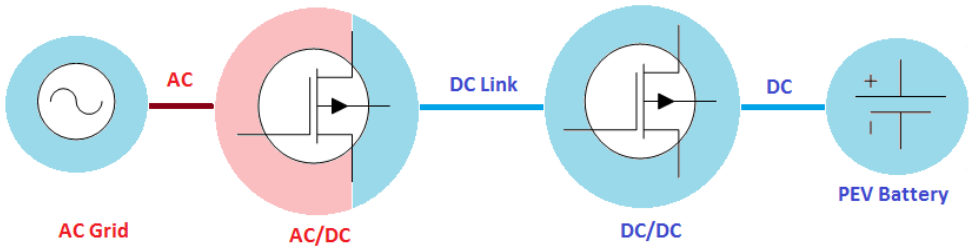

Figure 2-14:PEV battery charger structure [44]

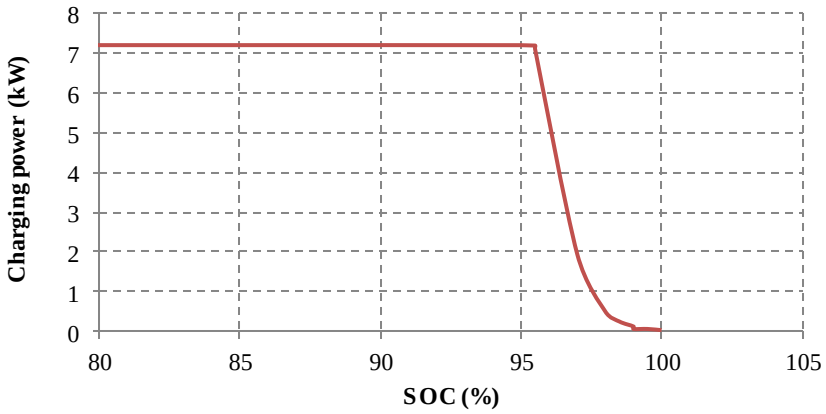

Figure 2-15: Li-ion battery characteristics [45]

2.4 Literature review

The work presented in this thesis focuses on optimal allocation of PEV parking lots in conjunction with RES and BESS units. This implies determining the optimal location and sizes of installation. Moreover, the work includes consideration of optimal

operating strategy of the allocated resources. A literature survey in the topic of research is presented below.

2.4.1 Optimal allocation of RES

Although RES are environmental friendly, the harvested power from them is characterized by highly uncertainty, as they depend on highly variable and uncertain quantities of wind speed and solar irradiance. Moreover, existing distribution networks are not designed to accommodate high penetration level of such generation [46]. Therefore, planning the location and sizes of renewable DG units is a complicated process, and should be performed as accurately as possible [46-48]. The optimal allocation of DG units is a very important topic, which gained high interest since early 2000's. Nowadays, the focus is to increase the intake of the distribution networks from the renewable DG units without jeopardizing the distribution system equipment.

The optimal DG allocation algorithm presented in [46-52] were developed with the goal of improving the voltage profile and reducing power losses on radial topology; however the work presented in [46-52] is based only on DG units with dispatchable output power and did not consider the intermittent nature of renewable based DGs output power. In [53], time-varying models for generation and loads are utilized for optimal DG allocation. However, modeling the renewable DG with one day of variable data is not sufficient to include the uncertainty associated with the output of such DG units. The work in [28] includes consideration of the uncertainty associated with renewable DG units, by using probabilistic models for both generation and loads. However, the work

does not study the effect of the binding constraints on the DG allocation and utilized only balanced systems, which does not reflect the practical case of distribution feeders, which are usually unbalanced systems. Moreover, the work assumed that all system customers have the same loading profile, which is not practical. In [54], the authors proposed a technique for optimal renewable DG units' allocation, taking into consideration smart control schemes. In [27] and [43], the authors introduced a multi-objective DG allocation algorithm to allocate renewable and dispatchable DG units in distribution networks. However, the work only includes consideration of balanced distribution networks. Multi-objective techniques for DG allocation are proposed in [55] and [56] to minimize losses and optimally allocate renewable DG units. In [57], the authors presented a DG allocation algorithm, which is based on Genetic Algorithm (GA). The proposed work in [57] can efficiently deal with distribution system topology changes in timely manner. However, the study did not include consideration of the uncertainty of renewable DG units' output power; besides, the run time is not a burden in these types of planning problems. The work in [58] presents an optimal DG allocation method to enhance the reliability of microgrid systems. The work includes consideration of the uncertainty associated with renewable DG output power, through utilizing probabilistic models for wind speed and solar irradiance. However, the work only included consideration of balanced systems.

The work in [46] to [58] focus on identifying the optimal location and sizes of DG units without studying the impacts of the binding constraints on the objective, where a change in these constraints might lead to increase of the DG intake with slight decrease in

the objective function, which can be preferred from the point of view of the distribution network operators (DNOs). Hence, a careful study of the effect of the binding constraints on the allocation of DG units is required. Moreover, most of the aforementioned studies assumed balanced distribution systems with same load profile for all customers, which do not reflect the practical situation of distribution systems [59].

2.4.2 Optimal allocation of BESS

The BESS allocation has been tackled in research to optimize several objectives, which include [36]:

- Deferring the network upgrades
- Peak demand shifting
- Enhancing the power system reliability

Several publications tackled the optimal operation of ESS, as in [60-62] in electricity markets. Another work addressed minimizing the annual capital and operational costs of a system composed of generation and storage facilities, as in [66]. However, this work didn't include consideration of the power network, i.e., the optimal location of the BESS was not considered.

The work in [67] proposed methods to investigate the impacts of high penetration of energy storage on the electricity market. However, the presented work didn't include a method to integrate an optimal operating strategy. Moreover, the work in [67] didn't include consideration of the optimal location of BESS.

The authors in [63] proposed a two-stage methodology for optimal allocation of storage units in distribution networks to improve the system reliability through successful islanding operation, which results in reduced interruptions of the power supply. The work in [64] proposed optimal sizing and siting of BESS to optimize overall costs of operating the distribution networks in regulating price or locational marginal price mechanisms. In [65, 66], the authors proposed optimal allocation of BESS to optimize several objectives, which include voltage profile, and losses. A probabilistic based technique is proposed in [67] to optimally allocate BESS in distribution systems with high penetration of wind based DG units. The aim was to maximize the benefits for the DG owners and the grid operators. The work in [68] proposed an optimal allocation of BESS to defer system upgrades and minimize system losses. However, the work in [68] was based on heuristic approach and didn't provide a complete mathematical model to the planning problem.

2.4.3 PEV charging stations planning

Although, PEV charging stations required to be carefully allocated in distribution networks, as these networks are not designed originally to accommodate this extra load, very few publication exist in the area of PEV charging stations allocation. As in [69], the authors proposed a technique to optimally allocate inductive charging stations and charging pads in distribution networks. However, the work included consideration of the EV traffic flows without considering the electrical system characteristics. In [70], a technique is proposed for allocation and energy scheduling of EV charging facilities, while implementing vehicle to grid (V2G) mechanism. However, similar to [69], the

work in [70] didn't consider the electrical system characteristics. The work in [71] proposes a method to optimally allocate EV charging stations taking into consideration customers' preferences into the location planning model. In [72], a multi-objective approach is used for optimal allocation of PEV charging stations while considering the traditional investment in network reinforcement as means of accommodating the PEV charging stations. A multi-stage approach is proposed in [73] to allocate PEV charging stations. The work includes consideration of several aspects, such as travel pattern, consumer behavior, road network, and grid limits. In [74], the authors proposed a method to optimally allocate PEV charging stations taking into consideration drivers' trip model. A methodology based on GA is proposed in [75] for the optimal allocation of PEV charging stations to improve the system reliability.

Some work included consideration of distribution system technical limits and grid impacts of allocating PEV charging stations, as in [76, 77]. In [76], the authors included preferences of PEV owners, who are likely to spend more time in certain locations, such as restaurant, stores, and shopping malls. An approach is developed in [77] and [78] to allocate the PEV charging stations in order to minimize the trips for charging stations.

The work in [79] considered optimal allocation of PEV charging stations based on game theory to maximize the social welfare. The methodology is proposed in [80] for optimal allocation of EV charging stations taking into consideration the AER range and the overall costs. The authors in [81] proposed an optimal allocation approach for PEV charging stations to minimize the overall costs.

In all previous work, the authors didn't include the probabilistic nature of PEV consumption, renewable resources generation, and normal demand of the distribution system.

Chapter 3
RES DG optimal allocation

This chapter investigates the impacts of binding constraints of the planning algorithms on the optimal allocation and sizing of renewable based DG units in distribution networks. The planning algorithm under study depends on developing multi-state probabilistic models for the distribution system components and combining these models in one comprehensive model that describes all possible system states. Several technical constraints are taken into consideration, including maximum reverse power at the substation, maximum number of renewable DG connections, voltage technical limits, thermal limits of cables and overhead lines, and voltage unbalance. In this work, the renewable DG allocation binding constraints are studied, where the effect of these constraints on the objective function, also known as shadow price, is investigated. The 123-bus unbalanced three phase IEEE test system has been utilized in a case study to show the effectiveness of the proposed algorithm. The renewable DG allocation problem is formulated as nonlinear mixed-integer programming and solved in general algebraic modeling system (GAMS) environment.

3.1 Introduction

The goal of the work presented in this chapter is to evaluate and quantify the impacts of the binding constraints on the optimal allocation and sizing of RES DG units with consideration of the following:

- Uncertainty due to the intermittent nature of renewable based DGs output power.
- Load variation and customer sector type.
- Unbalanced distribution networks.

Figure 3-1 depicts a schematic diagram of the proposed study. As shown in the figure, the proposed study starts by modeling the distribution system, the loads, and the renewable DG units. The planning problem is then formulated, with an objective function of minimizing the cost of energy losses. The problem will be subjected to several system constraints in order to make sure that the normal operating practices of the distribution system are not violated. The most salient constraints will be investigated versus the DG intake and the objective variations. The renewable DG allocation problem is formulated as a probabilistic nonlinear mixed-integer programming.

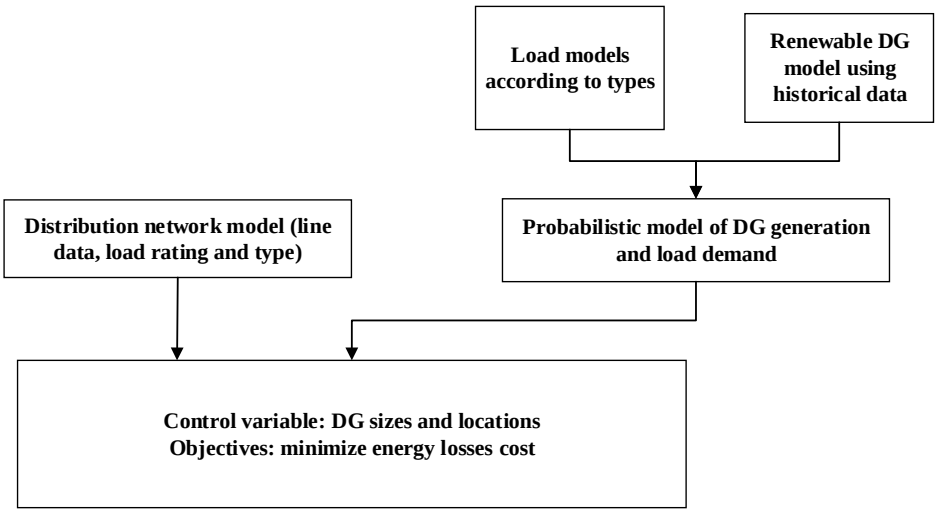

Figure 3-1: A brief description of the DG allocation approach.

3.2 Modeling

3.2.1 Renewable DG modeling

In this section, the probabilistic model of photovoltaic (PV) is presented. The same technique used to model PV based DG can also be used to model wind based DG. However, for a specific time segment, the solar irradiance data usually have a bimodal distribution function (pdf) [28]. Therefore, the data for each time segment are divided into two groups, each with a unimodal distribution function described by Beta probability density function [82]. On the other hand, the wind speeds usually follow a Weibull distribution function [28].

For this work, the solar irradiance for each hour of the day are modelled by Beta pdfs using six years of historical data from weather station located in Toronto, Ontario, Canada. The probabilistic model for the PV based DG units' output power is described as follows [43]:

- The entire year is divided into 12 months, and each month is being represented by a day within that month.
- The day which is representing the month is further subdivided into 24 one-hour segments each referring to a particular hourly interval of the entire month.
- The mean and standard deviation for each time segment are calculated utilizing the historical solar irradiance data.

- The Beta pdfs are generated for each hour using the mean and standard deviation for each segment.
- To describe the random phenomenon of the irradiance data, a Beta pdf is utilized for each unimodal [82].
- In order to integrate the output power of the PV modules as multistate, the continuous pdf of each is divided into a proper number of states, which is a trade-off between accuracy and computational time.
- Then, the probability of each irradiance state is calculated.
- Therefore, 24 pdfs (i.e., one pdf for each hour of the day hours) are developed for each month.
- The corresponding output power of the PV modules in each state are calculated using PV module characteristics [28].

3.2.2 Load modeling

The load in the distribution network under study is assumed to follow the three different load patterns [43]: residential, commercial, and industrial. Each type is modeled based on a defined number of states, depending on the desired accuracy, time scale, and speed of simulation, where the central centroid sorting process described in [83] is utilized to discretize the hourly load model. Each customer sector is assumed to follow same profile for each weekday and weekend in a specific month. This means that for each customer

sector, the load profile has 576 (12 month × 2 days × 24 hours) time segments, where each time segment has a unique pdf.

3.2.3 Combined generation-load model

This model describes all system states and their probabilities $\mathbb{p}_{(t,s)}$ that correspond to different generation and load states. For the generation of this model, the year is divided into 12 months, and each month is modeled by two days: weekday and weekend. For each time segment of the 576, the probability of each combined state is then calculated as the convolution of all the probabilities associated with that state, as in (3-1). The probability of the occurrence of each state $s \in \mathcal{S}_{sys}$ during any time segment is also evaluated, as in (3-2).

$$\mathbb{p}_{(t,s)} = \mathbb{p}_{(t,s_{PV})} \times \mathbb{p}_{(t,s_R)} \times \mathbb{p}_{(t,s_C)} \times \mathbb{p}_{(t,s_I)} \quad \textbf{(3-1)}$$

$$\mathbb{p}_{(s)} = \left(\frac{1}{576}\right) \times \sum_{t=1}^{576} \mathbb{p}_{(t,s)} \qquad \forall s \in \mathcal{S}_{sys} \quad \textbf{(3-2)}$$

3.3 Problem formulation

This section presents the DG allocation mixed integer nonlinear programming (MINLP) problem, which consists of the objective function and constraints, as follows:

$$\min \sum_{s} \sum_{ph1} \mathbb{p}_{(s)} \times 8760 \times C_{kWh} \times P_{loss\,(s,ph1)} \quad \textbf{(3-3)}$$

Subject to:

1) Power flow constraints

$$P_{inj\,(i,ph1,s)} = P_{G\,(i,ph1,s)} - P_{L(i,ph1,s)}$$

$$= \sum_{j \in \mathcal{S}_{bus}} \sum_{ph2 \in \mathcal{S}^{bus}_{ph(j)}} \left(V_{mag(i,ph1)} V_{mag(i,ph2)} Y_{mag(i,j,ph1,ph2)} \cos(Y_{ang(i,j,ph1,ph2)} + V_{ang(i,ph2)} - V_{ang(i,ph1)})\right) \quad \textbf{(3-4)}$$

$$- \left(V_{mag(i,ph1)} V_{mag(j,ph2)} Y_{mag(i,j,ph1,ph2)} \cos(Y_{ang(i,j,ph1,ph2)} + V_{ang(j,ph2)} - V_{ang(i,ph1)})\right) \; \forall i \in \mathcal{S}_{bus}, ph1 \in \mathcal{S}^{bus}_{ph(i)}$$

$$Q_{inj\,(i,ph1)} = Q_{G(i,ph1)} - Q_{L(i,ph1)}$$

$$= \sum_{j \in \mathcal{S}_{bus}} \sum_{ph2 \in \mathcal{S}^{bus}_{ph(j)}} \begin{pmatrix} V_{mag(i,ph1)} V_{mag(j,ph2)} Y_{mag(i,j,ph1,ph2)} \\ \sin\left(Y_{ang(i,j,ph1,ph2)} + V_{ang(j,ph2)} - V_{ang(i,ph1)}\right) \end{pmatrix} \quad \textbf{(3-5)}$$

$$- \left(V_{mag\,(i,ph1)} V_{mag\,(i,ph2)} Y_{mag\,(i,j,ph1,ph2)} \sin\left(Y_{ang\,(i,j,ph1,ph2)} + V_{ang\,(i,ph2)} - V_{ang\,(i,ph1)}\right)\right) \; \forall i \in \mathcal{S}_{bus}, ph1 \in \mathcal{S}^{bus}_{ph(i)}$$

2) Voltage technical limits

The voltage of the system has to be kept within maximum and minimum limits, which are typically ± 5-6% dependent on the system voltage level. Moreover, the voltage unbalance has to be kept below the maximum allowable limit

$$V_{min} \leq V_{mag\,(i,ph1,s)} \leq V_{max} \quad \textbf{(3-6)}$$

$$100 \times \frac{V_{mag\,(i,ph1,s)} - V_{AVG\,(i,s)}}{V_{AVG\,(i,s)}} \leq UV_{\max} \quad \textbf{(3-7)}$$

$$V_{AVG\,(i,s)} = \sum_{ph1} V_{mag\,(i,ph1,s)} / N_{ph(i)} \quad \textbf{(3-8)}$$

3) Lines thermal limits

The current flow in lines should not exceed the thermal capacity, as in **(3-9)**.

$$I_{mag\,(l,ph1)} \leq I_{\max(l,ph1)} \quad \textbf{(3-9)}$$

4) Generated powers constraints

It is assumed in this work that the renewable DG units operate at fixed power factor, which is assumed unity. Also, it is assumed that the total number of DG units installed in the system is limited to a maximum of N_{MAX}^{PV}.

$$P_{G\,(i,ph1)} = 0 \;\forall\; i \in \mathcal{S}_{no-GEN} \quad \textbf{(3-10)}$$

$$Q_{G\,(i,ph1)} = 0 \;\forall\; i \in \mathcal{S}_{no-GEN} \quad \textbf{(3-11)}$$

$$P_{G\,(i,ph1)} = a_{(i,ph1)} \times \mathscr{b}_{(i,ph1)} \times PV_{step} \;\forall\; i \in \mathcal{S}_{PV} \quad \textbf{(3-12)}$$

$$P_{G(i,ph1)} \leq PV_{MAX} \;\forall\; i \in \mathcal{S}_{PV} \quad \textbf{(3-13)}$$

$$Q_{G(i,ph1)} = 0 \forall\; i \in \mathcal{S}_{PV} \quad \textbf{(3-14)}$$

$$\sum_{i}\sum_{ph1} a_{(i,ph1)} \leq N_{MAX}^{PV} \quad \textbf{(3-15)}$$

5) Reverse power flow limit

According to the regulation of the distribution network operator, the reverse power flow at the substation should be limited to a maximum of 60% of the substation capacity [43].

$$\sqrt{P_{G\,(i=1,ph1)}{}^{2} + Q_{G\,(i=1,ph1)}{}^{2}} > 0.6 \times kVA_{SS}/3 \quad \textbf{(3-16)}$$

6) Losses constraints

$$P_{loss\,(ph1)} = \sum_{i} P_{G\,(i,ph1)} - P_{L(i,ph1)} \;\; \forall ph1 \quad \textbf{(3-17)}$$

$$Q_{loss\,(ph1)} = \sum_{i} Q_{G(i,ph1)} - Q_{L(i,ph1)} \;\; \forall ph1 \quad \textbf{(3-18)}$$

3.4 Sample case study

Consider the 123-bus IEEE test system under study in [84] which is unbalanced and contains a mix of residential, commercial and industrial customers being supplied from a common supply point, which is similar to the Canadian distribution as shown in Figure 3-2. The load and lines data are available in appendix A [84] .

Choosing the candidate buses for the DG allocation is complicated techno-economic problem, which is out of the scope of the presented study. Thus, all system buses are assumed to be candidate buses for the proposed work. The probabilistic model presented here is utilized to model the PV based DG units output power. Twenty states are assumed to represent the PV module output, where the outcomes of the clustering process are shown in Table 3-1. Moreover, the load is assumed to be of three types: residential, commercial, and industrial. It is assumed that 10 states represent each type. The outcomes of the load clustering process are shown in Table 3-2.

Table 3-1: PV based DG states as a percentage of capacity

Generation state	State as a percentage of DG capacity
1	0.00%
2	2.13%
3	4.82%
4	7.79%
5	11.05%
6	14.76%
7	18.49%
8	22.23%
9	26.22%
10	30.34%
11	35.18%
12	39.89%
13	44.49%
14	49.57%
15	55.08%
16	60.83%
17	67.08%
18	73.96%
19	81.74%
20	90.75%

Table 3-2 : Load states as a percentage of peak load

Load state	State as a percentage of peak load		
	Residential	Commercial	Industrial
1	37.45%	29.47%	2.90%
2	43.74%	4.21%	6.60%
3	49.75%	31.58%	25.00%
4	55.27%	44.21%	30.00%
5	61.87%	55.79%	44.00%
6	66.96%	73.68%	53.50%
7	72.48%	86.32%	60.00%
8	78.57%	90.53%	62.00%
9	84.60%	96.84%	75.00%
10	100.00%	100.00%	100.00%

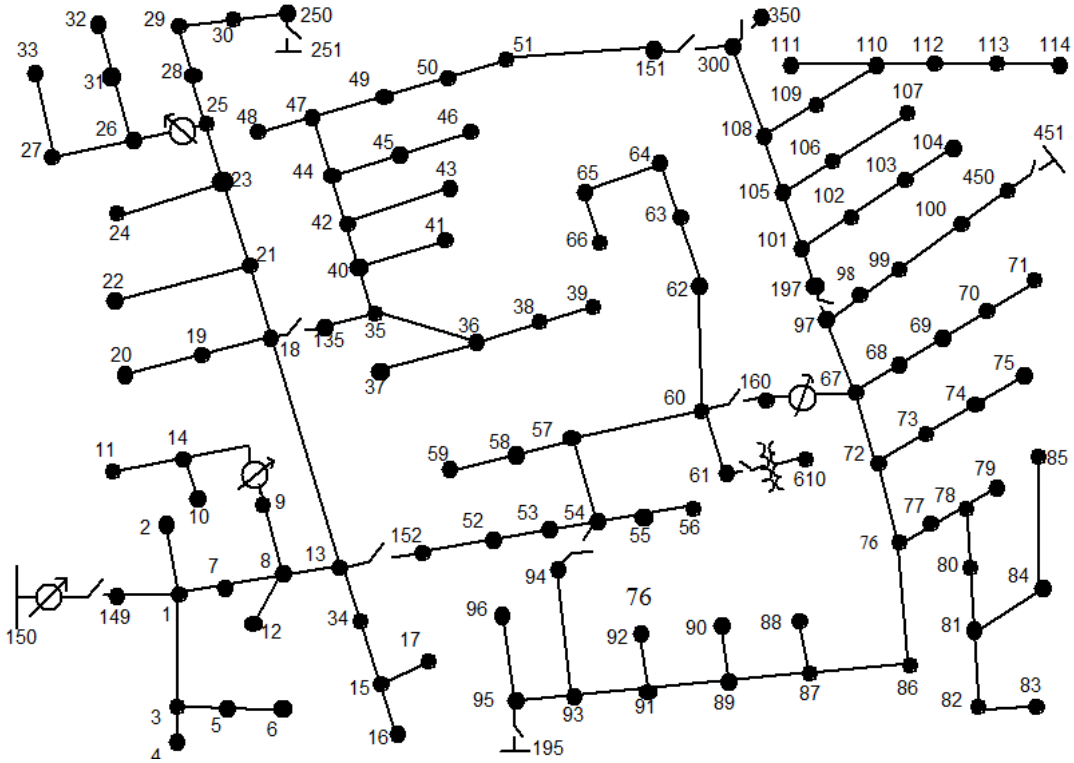

Figure 3-2: IEEE 123 node unbalanced test feeder [84]

Here it is noteworthy that only PV based DG units are utilized in this work; however, other types of renewable DG units, such as wind turbines can be utilized in same manner. For each customer type, the system buses are assigned as follows:

- Set of commercial customer buses: {2, 5, 7, 10, 15, 19, 22, 23, 25, 27, 33-35, 38-40, 42, 48, 55, 57, 58, 69, 70, 75, 77, 79, 80, 81, 83, 85, 86, 88, 91, 93, 94, 96, 98, 100, 104, 105, 106, 109, 110, 112, 113, 115, 119};
- Set of industrial customer buses: {52, 53, 54, 71, 72, 73, 82};
- The residential customer buses: All other buses.

Two cases are presented in this work representing base case, and optimal allocation. A detailed description of the results obtained in each case study is presented hereunder.

3.4.1 The base case results

For the base case, no DG units are considered. The price of energy is assumed to be 0.05 $/kWh. The total expected annual cost of the system energy losses is found to be $6533.4. This value corresponds to 130,668.7 kWh annual losses. These losses represent almost 3.24 % of the total kWh delivered to the customers.

3.4.2 DG allocation results

In this case study, the PV based DG units are allocated in the system. The outcomes of the DG allocation are shown in Figure 3-3, where PV_{step} is set to 5 kW, and the maximum number of DG units N_{MAX}^{PV} is set to very large number. Table 3-3 shows the total Installed capacity in kW on each phase where the total connected PV capacity is found to be 2,115 kW on the three phases a, b and c.

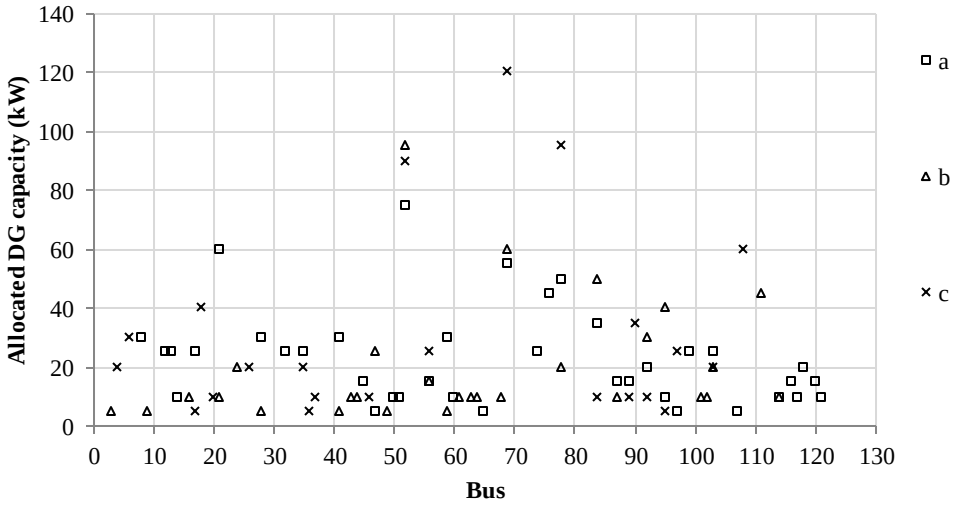

Figure 3-3: The outcomes of the DG allocation

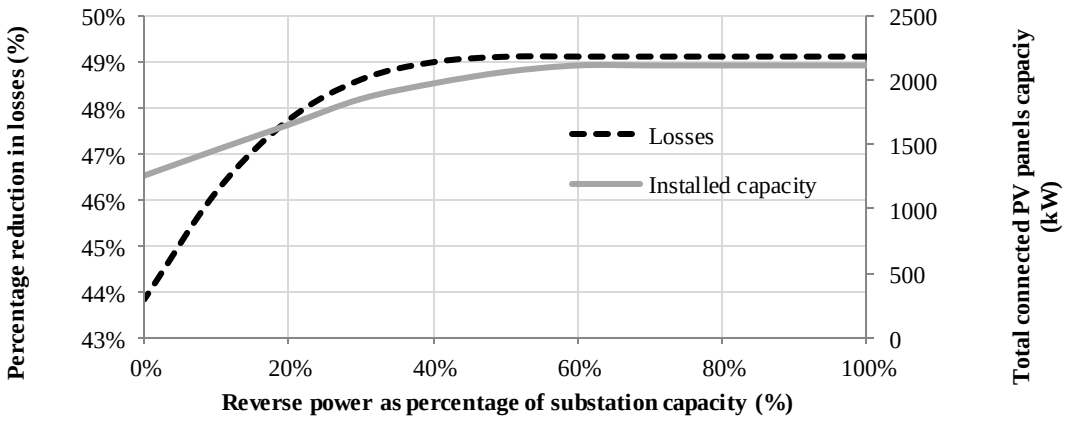

Figure 3-4: Effect of varying the reverse power flow limit

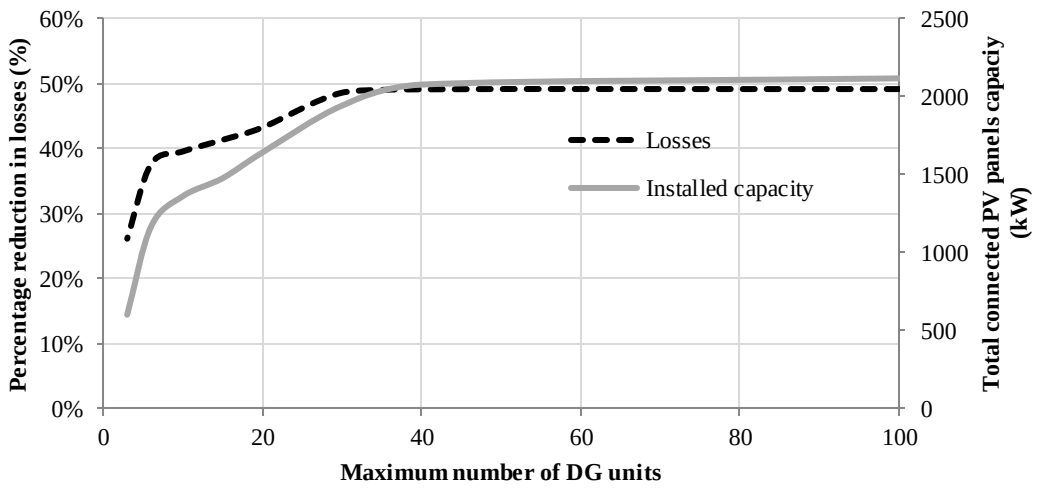

Figure 3-5: Effect of varying the maximum number of DG units installed in the system

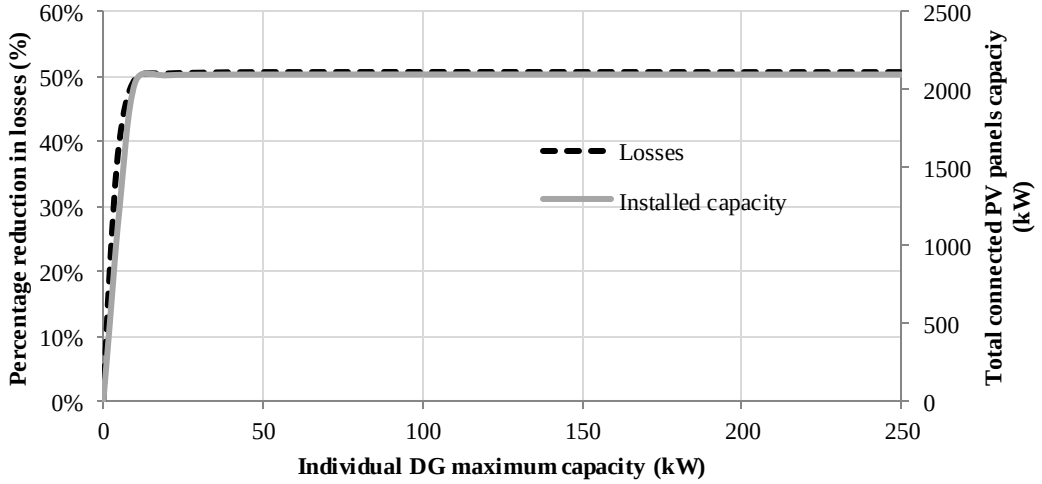

Figure 3-6: Effect of varying the maximum DG capacity

Table 3-3: Installed Capacities of DG units

Bus	Installed capacity in kW on each phase		
	a	b	c
Total (kW)	870	570	675

Moreover, the maximum allowable capacity per connection PV_{MAX} is limited to 200 kW. The corresponding total system losses are 66,492.6 kWh, which represents 49.11 % reduction in the system annual energy losses compared to the base case, which is very significant.

Further, to investigate the effect of varying the reverse power limit in (3-16), this limit is changed gradually to investigate its effect on the optimal sizes of DG units and the annual energy losses. As shown in Figure 3-4, limiting the reverse power flow to more than 60 % does not have significant effect on the allocated capacity or the losses reduction. This is due to the fact that the PV panels output cease during night, where normal load is minimum and the reverse power flow is expected to be significant. These results are system dependent, and are different for another system and/or another DG type. On the other hand, for reverse power limits lower than 60%, the allocated capacity keeps reducing and the losses reduction as well. For no reverse power allowance (0 % reverse power flow limit), the total losses reduction is 56.16 % and the total allocated PV panels capacity is 1,260 kW on all three phases, which is almost 59 % less than the capacity allocated with 60 % reverse power flow limit. Also, the results show that the constraint in (3-16) is almost binding just below the 60 % reverse power flow limit.

Moreover, the number of DG units N_{MAX}^{PV} in (3-15) is reduced gradually to study its effect on the allocation problem. As shown in Figure 3-5, when $N_{MAX}^{PV} > 40$ the constraint in (3-15) is not binding constraint and does not affect the losses or the installed capacity significantly. However, the slope of the increase in system losses gets steeper as

N_{MAX}^{PV} is reduced more. For example, when N_{MAX}^{PV} is reduced from 40 to 10, the reduction in the system losses is reduced from 49.11 % to 39.5 %. However, when N_{MAX}^{PV} is reduced from 10 to 3, the reduction in the system losses is reduced from 39.5 % to 26 %, where also (3-13) becomes binding. This can be noticed from the installed capacity, which is exactly 600 kW ($3 \times PV_{MAX}$).

Finally, the maximum capacity per PV based DG connection PV_{MAX} is changed to investigate its effect on the problem outcomes. As shown in Figure 3-6, for $PV_{MAX} > 10$ kW, no significant change occurs in the losses or the total installed capacity. However, the reduction in losses and the total installed capacity are reduced at high rate when PV_{MAX} is reduced below 10 kW. For example, when PV_{MAX} is reduced from 10 kW to 5 kW, the reduction in losses is reduced from 49 % to 39.8 %, respectively.

3.5 Discussions and conclusions

In this chapter, the optimal RES DG allocation problem is studied to quantify the impacts of binding constraints on the planning process of distribution systems. To that end, a probabilistic nonlinear mixed-integer planning problem is formulated. The generation and demand are individually modeled in probabilistic manner; then, different models are combined to generate a comprehensive multi-state probabilistic model that describes all possible system states. PV based DG units are considered in this work as the most promising renewable DG. The type of customers and unbalanced system, which reflect the practical situation of the grid, are modeled in the presented planning problem.

The study shows that optimal allocation of renewable DG units is very significant regarding energy losses reduction. Further, different aspects are studied regarding the effect of varying some of the salient constraints on the outcomes of the planning problem. By studying the effect of the reverse power flow limit at the substation, the 60 % limit imposed by Hydro One in Ontario, Canada is enough to reach the maximum possible intake of PV based DG units, as increasing this limit further does not result in significant increase in the total optimal allocated capacity in the system. Moreover, the maximum number of renewable DG units installed in the system has significant effect if reduced below certain limit, where this constraint becomes binding constraint. This limit is totally system dependent and can be extracted by varying the maximum number of DG units while keeping the other technical limits fixed. Furthermore, varying the maximum installed individual DG capacity also has significant effect on the DG allocation problem outcomes if reduced below certain threshold. Based on the outcomes and the analysis provided in this chapter, it is recommended to study the effect of the three studied technical limits on the outcomes of the allocation problem, as they have significant effect on the DG intake and the cost function reduction. Some of these technical constraints may be enhanced while the DG intake and the reduction in the cost of system losses are not affected, such as reducing the reverse power flow limit at the substation.

Chapter 4
RES and BESS optimal allocation in smart distribution power grid

The previous chapter focuses on optimal allocation of RES in distribution networks based on analytical probabilistic models. Chapter 4 extends the developed algorithm in the previous chapter to develop an approach for optimal allocation of RES and BESS units in distribution systems.

4.1 Introduction

The massive deployment of RES and BESS has gained significant interest in distribution networks, which creates a great challenge for distribution network investment planners and stakeholders. Toward this, an optimization problem formulation has been developed to determine the optimal locations and capacities of RES and BESS units in distribution systems. The objective of the proposed planning aims to minimize the overall capital and operational costs. For the purpose of accuracy, smart inverter control of renewable DG units and smart scheduling of BESS have been taken into consideration. The planning problem of determining the optimal location and sizes of RES and BESS units is formulated as MINLP.

4.2 Modeling

In this section the modeling of the system components (i.e. normal load, BESS, and RES) will be discussed. The previous chapter presented only the optimal allocation of renewable DG units in distribution networks, where an analytical probabilistic approach has been used to model RES and loads. However, due to the involvement of BESS, where the energy stored at any time segment is related to the energy stored in the previous time segment, chronological probabilistic models should be utilized in this work. Accordingly, a Monte Carlo simulation (MCS) is used in this chapter for modelling the distribution system components instead of analytical probabilistic models

4.2.1 Normal load modeling

The normal load model is assumed to follow the reliability test system (RTS) load pattern [85], where uncertainty of -5% to +5% is added as a uniform distribution to generate random scenarios of normal load.

4.2.2 RES generated output power modeling

RES output power should be modeled with proper pdf. The work in this thesis focuses on PV based RES, which are modeled using Beta pdf. However, the same model can be applied for wind based renewable DG units, where Weibull pdf is more suitable to fit the wind speed data [28]. The available historical data of solar irradiance for 6 years are clustered into four seasons, where each season is modeled as 24 hours. Thus, the model consists of 96 time segments. For each hour, proper pdf parameters are calculated, which

in this case Beta pdf. Then, MCS is used to generate a number of virtual scenarios, which mimic the history for the solar irradiance as shown in Figure 4-1. Finally, the simulated values of solar irradiance and average monthly temperatures are converted into output power based on the characteristics of the PV panels as discussed in 2.1.5.3.

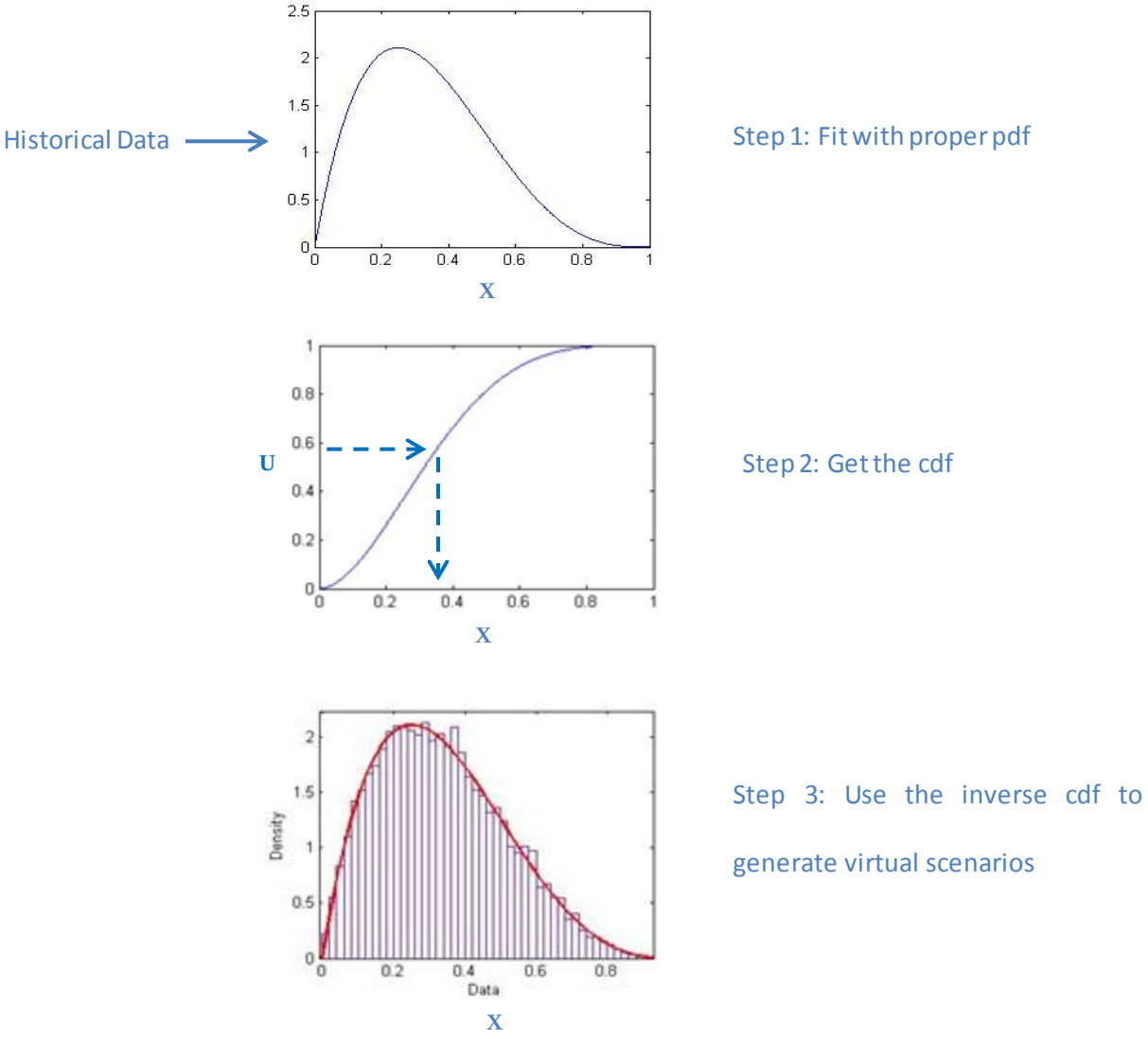

Figure 4-1: Generating virtual scenarios of RES generation

4.2.3 Battery energy storage systems

The BESS in this work is assumed to be four quadrants, as explained previously in 2.2.1 and shown in Figure 2-13. For simplicity, the BESS is modeled as a constant power demand or generation at any instant of time. Further, technical limitations on the stored energy, SOC level, charge/discharge rates, and reactive power limits are considered. The BESS receives two reference signals for active and reactive powers, which represent the decision variable of the optimal operating schedule of the BESS. The reference signals are different in the operation time horizon (i.e. from one hour to another) based on the system state. The detailed model is incorporated in the optimization problem formulation present below.

4.3 Problem formulation

This section presents the mathematical formulation of the proposed optimization-planning problem. The objective function of the planning problem including consideration of 1) the capital and operating cost of the new technologies (RES, BESS), 2) the cost of energy losses and consumed energy by normal load and BESS, and 3) the profit of selling energy from RES. The objective function is represented as follows:

$$\min_{\Omega} \sum_{s} \mathbb{p}_{(s)} \times (C_{PV} - G_{PV(s)} + C_{BES} + C_{Loss(s)} + C_{cons(s)}) \qquad \textbf{(4-1)}$$

where,

$$C_{PV} = \sum_{i} C_{PV/kW}\, P_{PV\_CAP(i,ph1)}\, /LV \tag{4-2}$$

$$G_{PV(s)} = G_{PV/kWh} \sum_{i} \sum_{ph1} \Bigg((N_{WD}/N_{tot}) \sum_{d \in \mathcal{WD}} \sum_{h} P_{PV(i,ph1,h,d,s)} + (N_{WE}/N_{tot}) \sum_{d \in \mathcal{WE}} \sum_{h} P_{PV(i,ph1,h,d,s)} \Bigg) \tag{4-3}$$

$$C_{BES} = \sum_{i} \sum_{ph1} \Big(C_{BES/kW}\, P_{BES\_kW(i,ph1)}\, /LV \; + (C_{BES_{OM}} + C_{\frac{BES}{kWh}}) P_{BES\_kWh(i,ph1)}\, /LV \Big) \tag{4-4}$$

$$C_{Loss(s)} + C_{cons(s)} = (C_{grid/kWh}\, /LV) \Bigg((N_{WD}/N_{tot}) \sum_{d \in \mathcal{WD}} \sum_{h} P_{grid(h,d,s)} + (N_{WE}/N_{tot}) \sum_{d \in \mathcal{WE}} \sum_{h} P_{grid(h,d,s)} \Bigg) \tag{4-5}$$

$$LV = \frac{(1 + r')^{LT} - 1}{r'(1 + r')^{LT}} \tag{4-6}$$

$$r' = \frac{r - f}{1 + f} \tag{4-7}$$

As shown in (4-1), the objective function of the planning problem depends on the decision variable set Ω, which contains the decision variables of installing the RES and BESS units , as well as, the decision variables of the operation scheduling including the active and reactive power absorbed/delivered by BESS and the active and reactive power

generated/curtailed by RES. Here it is worth noting that all the capital costs ($) are annualized or levelized ($/yr) by assuming that the capital investments are borrowed and paid annually with a fixed amount ($/yr). The costs of the system equipment are annualized as shown in (4-2) to (4-7) where the fixed capital costs are divided by the levelized cost (LV), which is expressed in terms of the interest rate (r), inflation rate (f), and lifetime of the equipment (LT) [23] .The objective function is subject to the following:

1) Power flow constraints

$$P_{inj(i,ph1,h,d,s)} = P_{G\,(i,ph1,h,d,s)} - P_{L\,(i,ph1,h,d,s)}$$

$$= \sum_{j \in \mathcal{S}_{bus}} \sum_{ph2 \in \mathcal{S}^{bus}_{ph(j)}} \left(V_{mag(i,ph1,h,d,s)} V_{mag(i,ph2,h,d,s)} Y_{mag(i,j,ph1,ph2)} \cos(Y_{ang(i,j,ph1,ph2)} \right.$$

$$\left. + V_{ang(i,ph2,h,d,s)} - V_{ang(i,ph1,h,d,s)})\right) \quad \textbf{(4-8)}$$

$$- \left(V_{mag(i,ph1,h,d,s)} V_{mag(j,ph2,h,d,s)} Y_{mag(i,j,ph1,ph2)} \cos(Y_{ang(i,j,ph1,ph2)} + V_{ang(j,ph2,h,d,s)} \right.$$

$$\left. - V_{ang(i,ph1,h,d,s)})\right) \; \forall i \in \mathcal{S}_{bus}, ph1 \in \mathcal{S}^{bus}_{ph(i)}, h, d, s$$

$$Q_{inj(i,ph1,h,d,s)} = Q_{G(i,ph1,h,d,s)} - Q_{L(i,ph1,h,d,s)}$$

$$= \sum_{j \in \mathcal{S}_{bus}} \sum_{ph2 \in \mathcal{S}^{bus}_{ph(j)}} \begin{pmatrix} V_{mag(i,ph1,h,d,s)} V_{mag(j,ph2,h,d,s)} Y_{mag(i,j,ph1,ph2)} \\ \sin\left(Y_{ang(i,j,ph1,ph2)} + V_{ang(j,ph2,h,d,s)} - V_{ang(i,ph1,h,d,s)}\right) \end{pmatrix} \quad \textbf{(4-9)}$$

$$- \left(V_{mag(i,ph1,h,d,s)} V_{mag(i,ph2,h,d,s)} Y_{mag(i,j,ph1,ph2)} \sin\left(Y_{ang(i,j,ph1,ph2)} + V_{ang(i,ph2,h,d,s)} \right.\right.$$

$$\left.\left. - V_{ang(i,ph1,h,d,s)}\right)\right) \; \forall i \in \mathcal{S}_{bus}, ph1 \in \mathcal{S}^{bus}_{ph(i)}, h, d, s$$

$$P_{G(i,ph1,h,d,s)} = P_{g-BES(i,ph1,h,d,s)} + P_{PV(i,ph1,h,d,s)} \quad \forall i \in \mathcal{S}_{bus}, ph1 \in \mathcal{S}^{bus}_{ph(i)}, h, d, s \quad \textbf{(4-10)}$$

$$Q_{G(i,ph1,h,d,s)} = Q_{g-BES(i,ph1,h,d,s)} + Q_{PV(i,ph1,h,d,s)} \quad \forall i \in \mathcal{S}_{bus}, ph1 \in \mathcal{S}^{bus}_{ph(i)}, h, d, s \quad \textbf{(4-11)}$$

2) Voltage technical limits

The voltage of the system has to be kept within maximum and minimum limits, which are typically ± 5-6% dependent on the system voltage level.

$$V_{min} \leq V_{(i,ph1,h,d,s)} \leq V_{max} \quad \forall i \in \mathcal{S}_{bus}, ph1 \in \mathcal{S}_{ph(i)}^{bus}, h, d, s \qquad \textbf{(4-12)}$$

3) Lines thermal limits

$$I_{(i,j,ph1,h,d,s)} \leq I_{MAX(i,j,ph1,d)} \quad \forall i \in \mathcal{S}_{bus}, ph1 \in \mathcal{S}_{ph(i)}^{bus}, h, d, s \qquad \textbf{(4-13)}$$

4) *Discrete size of DER constraints*

$$P_{BES\_kW(i,ph1)} = a_{BES(i,ph1)} \times \mathcal{b}_{BES1(i,ph1)} \times P_{BES-kW}^{Step} \quad \forall i \in \mathcal{S}_{bus}, ph1 \in \mathcal{S}_{ph(i)}^{bus} \qquad \textbf{(4-14)}$$

$$P_{BES\_kWh(i,ph1)} = a_{BES(i,ph1)} \times \mathcal{b}_{BES2(i,ph1)} \times P_{BES-kWh}^{Step} \quad \forall i \in \mathcal{S}_{bus}, ph1 \in \mathcal{S}_{ph(i)}^{bus} \qquad \textbf{(4-15)}$$

$$P_{PV\_CAP(i,ph1)} = a_{PV(i,ph1)} \times \mathcal{b}_{PV(i,ph1)} \times P_{PV}^{Step} \quad \forall i \in \mathcal{S}_{bus}, ph1 \in \mathcal{S}_{ph(i)}^{bus} \qquad \textbf{(4-16)}$$

5) *Candidate bus constraints*

$$a_{BES1(i,ph1)}, \mathcal{b}_{BES1(i,ph1)}, a_{BES2(i,ph1)}, \mathcal{b}_{BES2(i,ph1)} = 0 \ \forall i \in \mathcal{I}_{BES}, ph1 \in \mathcal{S}_{ph(i)}^{bus} \qquad \textbf{(4-17)}$$

$$a_{PV(i,ph1)}, \mathcal{b}_{PV(i,ph1)} = 0 \quad \forall i \in \mathcal{I}_{PV} \ ph1 \in \mathcal{S}_{ph(i)}^{bus} \qquad \textbf{(4-18)}$$

6) RES operational constraints

$$P_{PV(i,ph1,d,h,s)} = X_{P-PV(i,ph1,d,h,s)} \times P_{PV\_CAP(i,ph1)} \times P_{PV(d,h,s)}^{MCS} \quad \forall i, ph1 \in \mathcal{S}_{ph(i)}^{bus}, d, h, s \qquad \textbf{(4-19)}$$

$$Q_{PV(i,ph1,d,h,s)} = X_{Q-PV(i,ph1,d,h,s)} \times P_{PV(i,ph1,d,h,s)} \times \tan(\cos^{-1}(pf_{PV})) \quad \forall i, ph1 \in \mathcal{S}_{ph(i)}^{bus}, d, h, s \qquad \textbf{(4-20)}$$

7) Reverse power flow limit

According to the regulation of the distribution network operator, the reverse power flow at the substation should be limited to a maximum of 60% of the substation capacity [28].

$$\sum_{i\neq 1}\sum_{ph1}\left(P_{G(i,ph1,h,d,s)} - P_{L(i,ph1,h,d,s)}\right) \leq P_{MAX}^{Rev} \quad \forall h,d,s \tag{4-21}$$

8) BESS operation constraints

As mentioned in the previous section, the BESS receives two reference signals: P_{g-BAT} and Q_{g-BAT}. The constraint in (4-22) relates the stored energy in any time segment to the stored energy in the previous time segment. The constraint in (4-23) limits the stored energy to the maximum kWh capacity of the BESS. The delivered or absorbed active power at any time segment is related to the charging/discharging decisions as in (4-24). Other technical limitations are introduced in (4-25) to (4-27).

$$E_{BAT(i,ph1,h+1,d,s)} = E_{BAT(i,ph1,h,d,s)} + X_{P-BAT(i,ph1,h,d,s)} \times P_{BAT-MAX(i,ph1,h,d,s)} \; \forall i \in \mathcal{I}_{BES}, ph1 \tag{4-22}$$

$$E_{BAT(i,ph1,h,d)} \leq E_{BAT-MAX(i,ph1)} \; \forall i \in \mathcal{I}_{BES}, ph1 \tag{4-23}$$

$$P_{g-BAT(i,ph1,h,d,s)} = X_{P-BAT(i,ph1,h,d,s)} \times \frac{P_{BAT-MAX(i,ph1,h,d,s)}}{Eff_{BAT(i)}} \forall i \in I_{BAT}, ph1 \tag{4-24}$$

$$E_{BAT(i,ph1,h,d,s)} \geq 0.01 \times SOC_{BAT-MIN(i,ph1)} \times E_{BAT-MAX(i,ph1)} \forall i \in \mathcal{I}_{BES}, ph1 \tag{4-25}$$

$$P^2{}_{g-BAT(i,ph1,h,d,s)} + Q^2{}_{g-BAT(i,ph1,h,d,s)} \leq P^2{}_{BAT-MAX(i,ph1,h,d,s)} \tag{4-26}$$

$$Q_{g-BAT(i,ph1,h,d,s)} = X_{Q-BAT(i,ph1,h,d,s)} \times Q_{BAT-MAX(i,ph1,h,d,s)} \quad \textbf{(4-27)}$$

4.4 Sample case study and discussions

The proposed planning framework is tested using the 38-bus distribution system shown in Figure 4-2 [86]. Although the problem formulation is based on unbalanced three phase system, the approach is applied to a balanced system for simplicity and to facilitate analyzing the results. The system contains a mix of residential, commercial and industrial customers being supplied from a common supply point. The system data are given in appendix B and type of customers are given in [86]. The total system peak load is 4.37 MVA. The interest rate and the inflation rate are assumed to be 5% and 1% respectively. For the RES, in this case PV, the capital cost is 3,500 $/kW [87] and the lifetime is 20 years. The step size is assumed to be 5 kW. The LA batteries, as one of the most cost effective storage technologies, are used in this case study. The parameters of LA batteries are given in Table 4-1 [32]. It is worth noting that candidate PV bus locations are determined by detailed techno-economic planning analysis, which are outside the scope of the presented work and assumed to be inputs to this study. Therefore, all the system buses are assumed to be candidate for the PV and BESS connections.

Table 4-2 shows a description of several case studies that have been conducted as a means of evaluating the merits of the proposed planning framework.

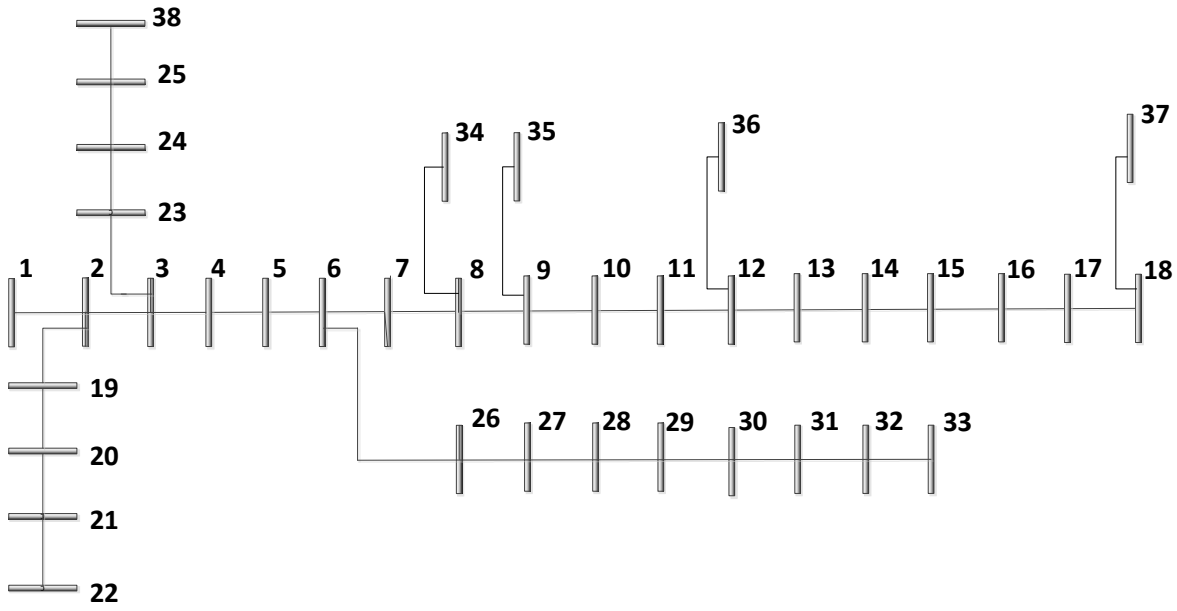

Figure 4-2: The 38-bus distribution test system

Table 4-1: Data of LA battery [32]

Power capital cost	175 $/kW
Energy capital cost	305 $/kWhr
Annual operation and maintenance cost	15 $/kW
Round-trip efficiency	75%
Life-time	3200 cycles
Maximum battery size	1000 kW – 1000
$P_{BES-kW}^{Step}, P_{BES-kWh}^{Step}$	25 kW, 25 kWh

Table 4-2: Description of the conducted case studies

Case	Description	Case	Description
A	Base case	***B***	PV DG allocation
C	BESS allocation	***D***	PV DG and BESS allocation

Table 4-3 shows the detailed simulation results of the cost of consumed energy and losses, the expenses of installations for PVs, and BESSs, and the profits achieved for the installations in each case study. Table 4-4 presents the optimal number, sizes and locations of the installed PVs, and BESS for each case study. As shown in Table 4-3, the total annual cost of the energy purchased from the grid in the base case (A), where no allocation is performed, is $1.320 M. This energy is the sum of the energy consumed by normal load customers and the energy dissipated as losses with contributions of 97.4 % and 2.6 % respectively. In case *B*, where only the allocation of PV is considered, it is assumed that the generated energy is sold to the grid at a fixed rate, which represents the incentives from the government to reduce the greenhouse gas emissions. The allocated capacity varies depending on the tariff at which the generated energy is sold. As shown in Figure 4-3, the profit of installing PV in the system is negative up to around 14.1 ¢/kWh. However, for a tariff above 12.5 ¢/kWh, the sum of the savings in the cost of energy losses and the negative profit is positive; thus, the planning problem starts allocating PV units in the system although the cost of installation is higher than the profit of selling energy to the grid. In this work, the feed-in-tariff (FIT) program in Ontario, Canada, is

used as a reference for a 27.5 ¢/kWh [31]. The total allocated capacity in this case is 4 MW, which represents the maximum allowable allocated capacity of DG units in the system. The allocation results in 30.4 % reduction in the annual energy losses and 53.8 % reduction in the cost of energy losses. This is due to the reduction of the losses in periods of high price. As shown in Table 4-3, the annual profit of selling energy to the grid is 90.8 % higher than the annualized installation cost of the PV. The net expenses to run the system are 72 % lower than the base case.

In case C, the allocation of the BESS resulted in a saving of 20.9 % in the cost of energy losses, and an annual profit of $51,457 due to price differences of energy from peak to off-peak periods. The net expenses to run the system are 1.6 % lower than the base case. The allocated BESS is at bus 31 with a capacity of 200 kW and 875 kWh. As shown in Figure 4-3, which shows one scenario of BESS charging/discharging schedule, The BESS starts charging when the prices are low till 8:00 am. Then, when the energy prices gets higher, it starts discharging from 8:00 am till 11:00 am and holds the stored energy till the prices drop at 12:00 noon. Case *D* considers allocating both PV and BESS. The total allocated capacity of PV is found to be 3,165 kW. On the other hand, one BESS unit is allocated at bus 38 with capacity of 625 kW and 3500 kWh. The reduction in the cost of energy loss is 77.8 %, which is very high due to smart scheduling of the BESS unit. Compared to the base case, the net expenses are 75.9 % lower.

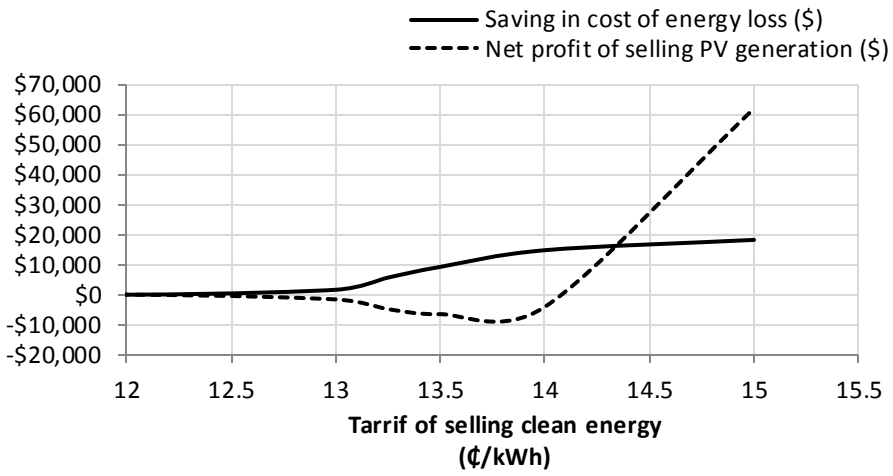

Figure 4-3: PV DG allocation saving and profit

Table 4-3: Cost related results

Case		*A*	*B*	*C*	*D*
Consumed energy	**($)**	1,286,360	1,286,360	1,286,360	1,286,360
	(%)*	0.00%	0.00%	0.00%	0.00%
Energy loss	**($)**	33,880	15,655	26,800	7,511
	(%)*	0.00%	-53.79%	-20.90%	-77.83%
Expenses ($)	**RES**	0	1,026,543		1,026,543
	BESS	0	0	37,519	143,397
Profit ($)	**RES**	0	1,959,130	0	1,959,130
	BESS	0	0	51,457	187,252
Net Expenses	**($)**	1,320,240	369,428	1,299,222	317,429

* Percentage increase from base case

Table 4-4: Technical results

Case		*A*	*B*	*C*	*D*
Losses	**(MWh)**	427	297	663	959
	(%)*	0.00%	-30.44%	55.27%	124.59%
RES allocation	**Bus**	–	5, 6, 8, 9, 10, 11, 12, 13, 14, 15, 16, 17, 18, 21, 22, 24, 25, 26, 27, 28, 29, 30, 31, 32, 33, 34, 37	–	4, 5, 6, 7, 10, 11, 12, 13, 16, 17, 18, 20, 23, 24, 25, 26, 29, 30, 31, 32, 38
	(kW)	–	5, 150, 125, 30, 75, 115, 190, 190, 275, 120, 180, 130, 155, 15, 35, 160, 335, 30, 20, 30, 110, 600, 275, 545, 85, 5, 15	–	90, 20, 215, 25, 75, 80, 165, 160, 125, 120, 130, 50, 25, 565, 505, 55, 125, 505, 60, 50, 30
BESS allocation	**Bus**	–	–	31	38
	(kW)	–	–	200	625
	(kWh)	–	–	875	3500

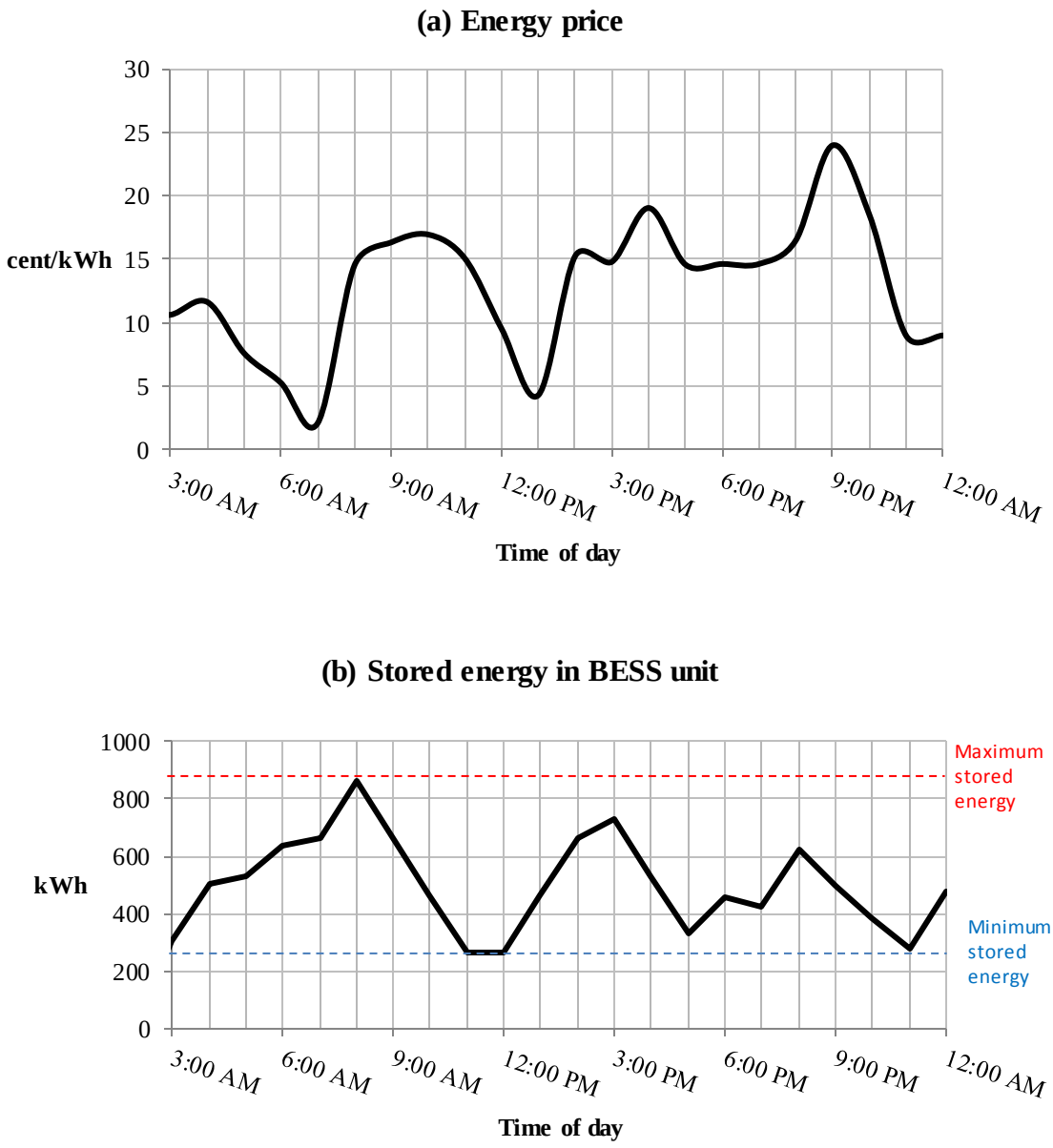

Figure 4-4: Energy prices and stored energy for a scenario from case *C*

4.5 Conclusions

This chapter presents a planning approach to allocate RES and BESS units in distribution networks. The presented approach can help the distribution companies and investors to optimize their investments. The proposed planning approach includes smart scheduling of the BESS units, and smart control of PV inverters. The planning problem is defined as MINLP, which is solved using deterministic optimization tool. Simulation results on a typical distribution system demonstrate that significant profit can be achieved by allocating BESS units in addition to renewable DG units. Although the results are entirely system dependent, the proposed method is generalizable and can be applied to any distribution network.

Chapter 5
PEV charging stations optimal allocation in smart power distribution grid

In this chapter, the previous work in chapter 4 is extended to include PEV parking lots allocation in conjunction with RES and BESS optimal allocation.

5.1 Introduction

This chapter presents the core of this thesis, which is presented by a conceptual framework and a methodology for optimal sizing and siting of grid-interfaced PEV chargers in parking lots in combination with RES and BESS in distribution networks. Unlike previous works, the proposed framework is more comprehensive, where the planning problems of PEVS, RES, and BESS all are combined together. To that end, a MINLP optimization planning problem formulation has been developed. The objective of the developed optimization problem is to achieve the minimum cost and maximum efficiency for local distribution companies and their stakeholders. The formulated problem accounts for the uncertainty due to the intermittent nature of RES output power and PEV charging load. In this regard, a new modeling for PEVs charging demand is proposed. Moreover, compared with previous works, the proposed framework is more accurate, where optimal operation scheduling of PEVs, RES and BESS has been incorporated in the formulated planning problem. Due to its complexity, the global optimization-planning problem has been split into two nested layers (sub-problems);

namely exterior and interior. The exterior layer represents the installation problem and it contains the solution space of the number, location and sizes of PEVs, RES and BESS; while, the interior layer determines the operation schedules of PEVs charging, RES and BESS for each candidate solution in the exterior layer. A combination between metaheuristic and deterministic optimization techniques has been utilized to solve the exterior and interior problems concurrently.

5.2 Modeling

In this section the modeling of the PEV demand is discussed. The normal load, BESS, and RES models are the same as in chapter 4.

Unlike previous models, which adopted rigid charging schedules for coordinated PEV charging, the proposed model utilizes historical data to generate virtual scenarios of vehicles arrivals and departures. These scenarios are later converted to energy consumption during the planning problem.

Since, each type of parking lots (residential, commercial down town, commercial commute, etc.) has unique arrival rates and parking durations, a generalized model is developed in this section, which utilizes MCS to generate virtual scenarios for PEV arrivals and parking durations. The output of this model can be described as virtual scenarios of PEVs charging, which are further translated to power consumption from the grid in the optimization process. Here it is worth noting that the power demand of PEVs depends on the charging mode of operation (i.e. uncoordinated or coordinated/scheduled) considered in the planning problem.

To generate this model, two major variables have to be considered, which affect the PEV coordinated load model in a parking lot; they are arrival rate and parking duration. The proposed model utilizes practical historical data of arrival rates and parking durations of conventional vehicles in several parking lots in Toronto, Ontario, Canada. These data are made available through Toronto Parking Authority. However, due to the lack of PEVs charging data, the required charging energy and charging rates limits are assumed to follow standard uniform distribution between minimum and maximum values. These two values are chosen based on the available PEVs in the market [1]. The proposed PEV model is illustrated in Figure 5-1, and can be described as follows:

Step 1: Each season of the year is modeled with two days: weekend (or holiday), and weekday. Consequently, the historical data is clustered into seasons, and each season data is clustered into weekday or weekend.

Step 2: The arrival rates in each of the 24 hours of the eight days (4 seasons × 2 days) representing the year are extracted from the historical data. Different types of pdfs are used to fit the arrival data. For instance, the arrival rates of the PEVs to a parking lot located in downtown Toronto are found to be modelled as Gaussian distribution. Therefore, for each of the eight days representing the year, there are 48 parameters (24 h × 2 parameters), i.e. mean and variance, are calculated from the historical data of the arrival rates.

Step3: For each hour of the 192 hours (24 h × 8 days) representing the year, the inverse of the Gaussian distribution of each cumulative distribution function (cdf) is used to generate *Ns* virtual scenarios of PEV arrivals, as in (1).

$$A_{(d,h,s)} = CDF^{-1}_{A(d,h)}\left(U_{(s)}\right) \qquad \forall d,h,s \leq N_s \tag{5-1}$$

Step 4: Virtual parking durations are generated for all vehicles in all scenarios for hour h in day d, as follows:

$$T_{(d,h,v)} = CDF^{-1}_{T(d,h)}\left(U_{(v)}\right) \qquad \forall d,h,\leq N_{VH(h)} \tag{5-2}$$

Step 5: As stated before, due to the lack of PEVs charging data, the numbers of PEVs arriving each hour for different scenarios are assigned random required charging energy and charging rate limit values according to uniform standard distribution. Hence, the parking duration, required charging energy, and charging rate, are defined for each PEV arrives to the parking lot in any scenario s.

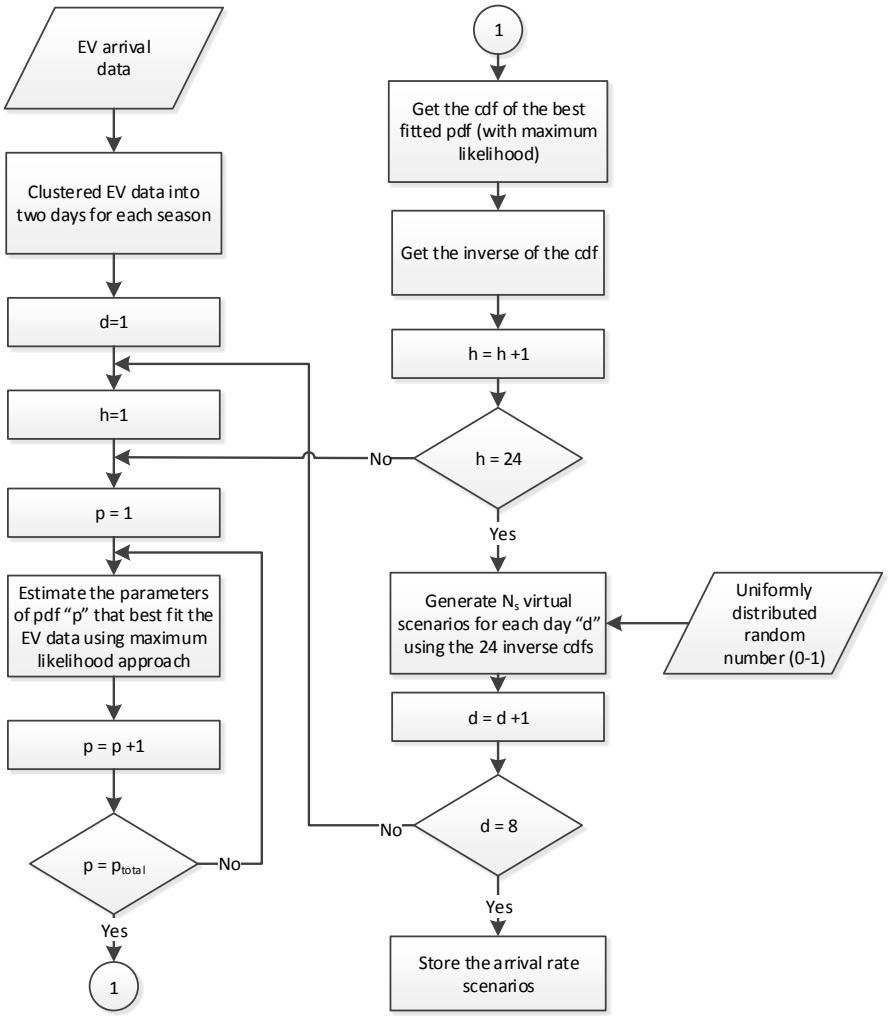

Figure 5-1: Proposed PEV arrival rate modeling

5.3 Problem formulation

This section presents the mathematical formulation of the optimization-planning problem. The objective function of the planning problem including consideration of 1) the capital and operating cost of the new technologies (PEVs, PV, BESS), 2) the cost of energy

losses and consumed energy by normal load, PEVs, and BESS, and 3) the profit of selling energy from PV. The objective function is represented as follows:

$$\min_{\Omega_1,\Omega_2} \sum_{s} \mathbb{p}_{(s)} \times (C_{PV} - G_{PV(s)} + C_{BES} + C_{EV} + C_{Loss(s)} + C_{cons(s)}) \quad \textbf{(5-3)}$$

where, all costs are as in (4-2) to (4-7) and

$$C_{EV} = C_{EV\_CH}\, N_{EV\_CH(i)}\, /LV \quad \textbf{(5-4)}$$

As shown in (5-3), the objective function of the planning problem depends on two decision variable sets (Ω_1 and Ω_2). The set Ω_1 contains the decision variables of the installation problem, i.e. $\Omega_1 = \{ a_{BES}\ , a_{PV}, b_{BES1} b_{BES2}, b_{EV}, b_{PV} \}$. On the other hand, the set Ω_2 contains the decision variables of the operation scheduling including the active power consumed by PEVs, the active and reactive power absorbed/delivered by BESS and the active and reactive power generated/curtailed by PVs, i.e. $\Omega_2 = \{ X_{P-BAT}, X_{Q-BAT}, X_{P-PV}, X_{Q-PV}, X_{EV} \}$. The objective function is subject to the same constraints in chapter 4, except for these changes or additions:

1) Power flow constraints

The power flow constraints are the same as in chapter 4. However, the demand on each bus includes the PEV consumption, i.e.

$$P_{L(i,ph1,h,d,s)} = P_{NL(i,ph1,h,d,s)} + P_{PEV\,(i,ph1,h,d,s)} \quad \forall i, ph1, h, d, s \quad \textbf{(5-5)}$$

2) *Candidate bus constraints*

$$\mathscr{b}_{EV(i)} = 0 \quad \forall i \in \mathcal{I}_{EV} \tag{5-6}$$

3) PEV operational constraints:

Based on the number of charging stations, i.e. $\mathscr{b}_{EV\,(i)}$, the PEV demand can be expressed in terms of the charging decision of vehicles v ($X_{EV(i,d,h,s,v)}$) as in (5-7) and (5-8). The maximum allowable rate of charge for each vehicle v is formulated as a function of the SOC as in (5-9). The total energy delivered for each vehicle is evaluated as in (5-10) and (5-11). The constraints in (5-12) relate the SOC of each vehicle v to the SOC in the previous time step.

$$P_{PEV(i,ph1,d,h,s)} = \sum_{v} \frac{X_{EV(i,ph1,d,h,s,v)}\ P_{CH(i,ph1,d,h,s,v)}}{\eta_{CH}} \tag{5-7}$$

$$P_{CH(i,ph1,d,h,s,v)} = \begin{cases} P^{max}_{CH(i,ph1,d,h,s,v)} & \forall P^{max}_{CH(i,ph1,d,h,s,v)} \le P^{capcity}_{CH(i,ph1,d,h,s,v)} \\ P^{capcity}_{CH(i,ph1,d,h,s,v)} & \forall P^{max}_{CH(i,ph1,d,h,s,v)} > P^{capcity}_{CH(i,ph1,d,h,s,v)} \end{cases} \tag{5-8}$$

$$P^{max}_{CH(i,ph1,d,h,s,v)} = f^{CH}_{(i,ph1,d,h,s,v)}\left(SOC_{(i,ph1,d,h,s,v)}\right) \tag{5-9}$$

$$E_{D(i,ph1,d,s,v)} = E_{BAT(i,ph1,d,s,v)} \sum_{h} \left(SOC_{(i,ph1,d,h,s,v)} - SOC_{(i,ph1,d,h-1,s,v)}\right)/100 \tag{5-10}$$

$$E_{D(i,ph1,d,s,v)} = E_{REQ(i,ph1,d,s,v)} \tag{5-11}$$

$$SOC_{(i,ph1,d,h,s,v)} = SOC_{(i,ph1,d,h-1,s,v)} + 100 \times \frac{X_{EV(i,ph1,d,h,s,v)}\ P^{max}_{CH(i,ph1,d,h,s,v)}}{E_{BAT(i,ph1,d,s,v)}} \tag{5-12}$$

5.4 PROBLEM SOLUTION

The formulation described in the previous section is a mixed integer nonlinear programming MINLP problem. To lower its complexity, the problem is split into two nested parts i.e. exterior and interior. The exterior and interior parts represent the installation and operation-scheduling problems, which are controlled by the decision variable sets, Ω_1 and Ω_2, respectively. Figure 5-2 shows a flowchart that summarizes the proposed solution mechanism of the formulated planning problem. As shown in the figure, a combination between metaheuristic technique and deterministic technique has been utilized to manage exterior and interior parts concurrently. The GA toolbox under the Matlab® environment is used as the metaheuristic technique, which governs the exterior part by determining the decision variable set Ω_1. As depicted in the figure, the interior NLP problem describing the operation scheduling is solved for an initial population of Ω_1 using a powerful commercial optimization software (GAMS environment) for each hour of the 8 days representing the year, and for each possible scenario *s*. The solution of the interior part yields the set of decision variables for the operation scheduling, i.e. Ω_2. Then, based on Ω_1 and Ω_2, the total capital and operational costs are calculated for each scenario.

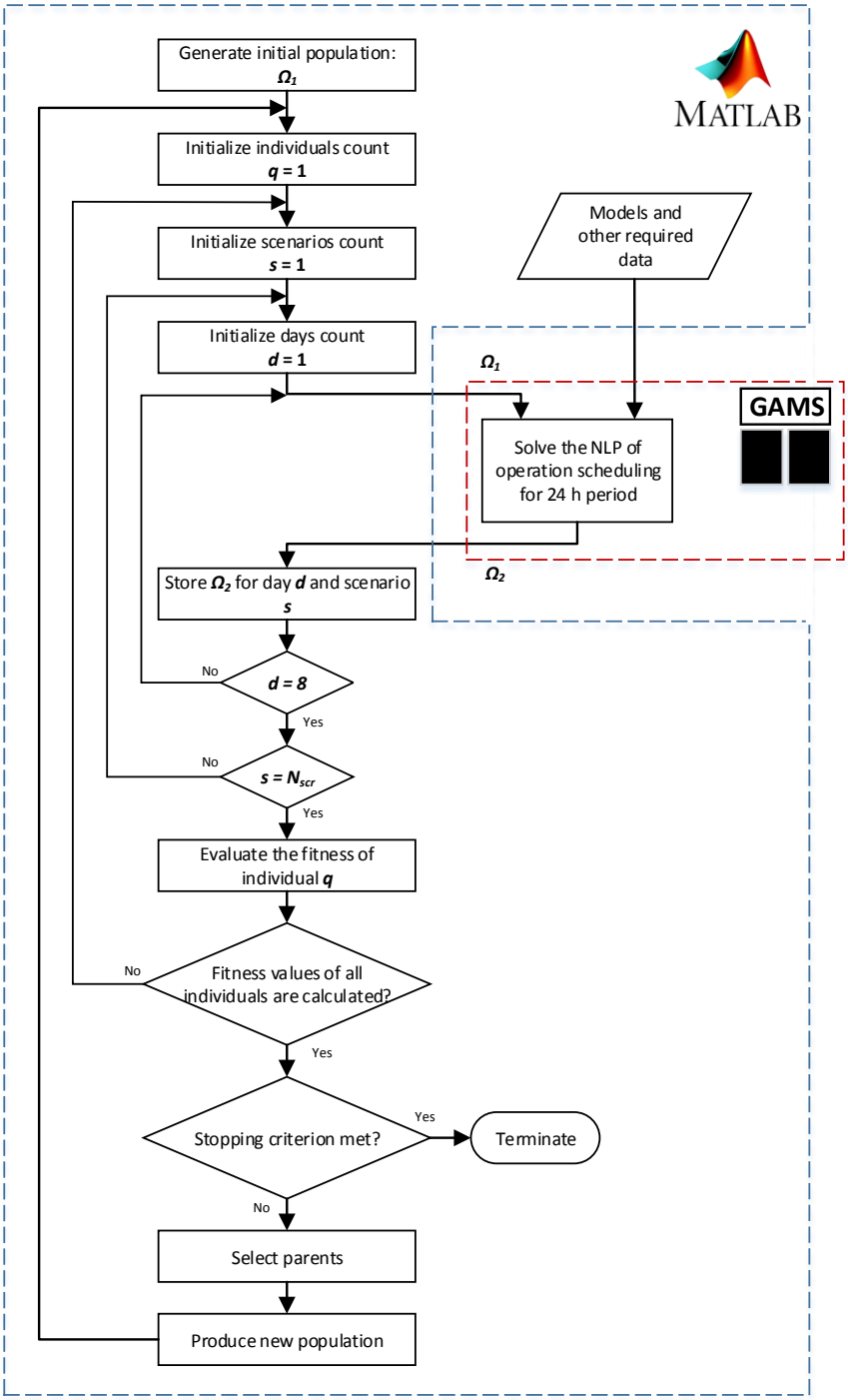

Figure 5-2: Proposed planning algorithm structure

The fitness of each individual, i.e. Ω_1, is defined as the overall expected costs or the overall system annualized costs. The overall annualized costs consist of the capital and operating costs of PEV charging stations, PVs, and BESS and the cost of purchasing energy from the grid, which includes the energy losses and consumed energy. Based on the fitness of each individual in the population, the stopping criterion is checked. If the stopping criterion is met, the approach terminates and the best individual is stored. If the stopping criterion is not met, the parents are selected through choosing elite child(s), crossover, and mutation. Then, a fitness proportionate selection is used to produce the new population of Ω_1

5.5 Sample case study and discussions

The proposed planning framework is tested using the 38-bus distribution system described in 4.4 and shown in Figure 4-2. All the information in 4.4 about the RES and BESS units is utilized in this work. The interest rate and the inflation rate are assumed to be 5% and 1% respectively [32]. The PEV chargers rating utilized in this study are 208-240Volt AC - 7.2kW 30Amp [43]. The price for a single pedestal charger is assumed to be $2,000 and the labour, permits, and material is$2,000 per charger. The installation cost for a single or double pedestal charger is assumed to be 1,000$. The PEV battery ratings are normally distributed between a minimum of 24 kWh to a maximum of 65 kWh. The PEV charging price is assumed to be flat at 0.35 $/kWhr. All the system buses are assumed to be candidate for the PV and BESS connections. However, for the PEV

charging stations busses 29 to 38 are only assumed as candidate buses arbitrary to reflect the locations of possible PEV chargers installation. Table II shows a description of a number of case studies were conducted as a means of evaluating the merits of the proposed planning framework. Table 5-1 shows the detailed simulation results of the cost of consumed energy and losses, the expenses of installations for PEVs, PVs, and BESSs, and the profits achieved for the installations in each case study.

Table 5-1: Description of the conducted case studies

Case	Description	Case	Description
A	Base case	***B***	PV DG allocation
C	BESS allocation	***D***	PV DG and BESS allocation
E	PEV stations allocation	***F***	PEV stations and PV DG allocation
G	PEV stations and BESS allocation	***H***	PEV stations, PV DG, and BESS allocation

Table 4-3 and Table 4-4 present the total annual cost and the optimal number, sizes and locations of the installed PVs, and BESS for cases A, B, C, and D. These results are also presented in Table 5-2 and Table 5-3, in addition to cases E, F, G, and H.

For the PEV stations allocation in case E, since it is extra load, the planning problem will only allocate these stations if the profit is higher than the sum of the cost of installation and the increase in the energy losses. The maximum allowable PEV charging stations in the system are 2.5 MW, which represents 285 chargers of level 2. The price of charging PEVs is assumed to be the base energy price plus a fixed profit to cover the capital costs,

operating costs, and cost of increased energy loss. For a fixed profit up to 3.25 ¢/kWh, the planning problem doesn't allocate any chargers. For a fixed profit of 4 ¢/kWh, the planning problem allocated 285 chargers, as shown in Table 5-2, where the cost of energy purchased from the grid and consumed by the customers is increased by 14.96 % and the energy loss is increased by 20.9 %. The total expenses to run the system are 2.6 % lower than the base case.

For case *F*, the PV units' installations are allowed to support PEV charging stations. As shown in Table 5-3, a total capacity of 4,000 kW of PV is installed in the system, which reduces the cost of energy loss by 48.8 % compared to case E, and 35.3 % compared to the base case. The net expenses are 74.7 % less than the base case. In case G, the planning problem allocates BESS to support the PEV charging stations. Although, the allocated capacity of BESS is 3,000 kW and 5,000 kWh, the cost of energy loss are still 18.8 % higher than the base case, but 1.8 % lower than case *E*. The net expenses are 18.1 % lower than the base case. For case H, the PV and BESS installation is allowed to support the PEV charging stations. However, the results show only PV allocated in the system, same as case F. This is due to two reasons. 1) The fact that the PV generation pattern fits PEV charging pattern in commercial lots, while residential PEV charging patterns can easily be shifted to low normal demand period at night, which doesn't need support from BESS units. 2) The incentives from governments for clean energy from PV give superiority for PV allocation in the system compared with much lower profit for allocating BESS units.

Table 5-2: Cost related results

Case		*A*	*B*	*C*	*D*	*E*	*F*	*G*	*H*
Consumed energy	**($)**	1,286,360	1,286,360	1,286,360	1,286,360	1,467,436	1,478,122	1,600,843	1,478,122
	(%)*	0.00%	0.00%	0.00%	0.00%	14.08%	14.91%	24.45%	14.91%
Energy loss	**($)**	33,880	15,655	26,800	7,511	40,980	21,914	40,250	21,914
	(%)*	0.00%	-53.79%	-20.90%	-77.83%	20.96%	-35.32%	18.80%	-35.32%
Expenses ($)	**RES**	0	1,026,543		1,026,543	0	1,026,543	0	1,026,543
	BESS	0	0	37,519	143,397	0	0	257,683	0
	EV chargers	0	0	0	0	162,092	162,092	162,092	162,092
Profit ($)	**RES**	0	1,959,130	0	1,959,130	0	1,959,130	0	1,959,130
	BESS	0	0	51,457	187,252	0	0	461,441	0
	EV chargers	0	0	0	0	384,315	395,001	517,722	395,001
Net Expenses	**($)**	1,320,240	369,428	1,299,222	317,429	1,286,193	333,587	1,081,705	334,540

* Percentage increase from base case

Table 5-3: Technical results

Case		*A*	*B*	*C*	*D*	*E*	*F*	*G*	*H*
Losses	**(MWh)**	427	297	663	959	738	369	1042	369
	(%)*	0.00%	-30.44%	55.27%	124.59%	72.83%	-13.58%	144.03%	-13.58%
RES allocation	**Bus**	–	5, 6, 8, 9, 10, 11, 12, 13, 14, 15, 16, 17, 18, 21, 22, 24, 25, 26, 27, 28, 29, 30, 31, 32, 33, 34, 37	–	4, 5, 6, 7, 10, 11, 12, 13, 16, 17, 18, 20, 23, 24, 25, 26, 29, 30, 31, 32, 38	–	6, 7, 8, 9, 10, 11, 12, 13, 14, 15, 16, 17, 18, 22, 24, 25, 26, 27, 28, 29, 30, 31, 32, 33, 34, 38	–	6, 7, 8, 9, 10, 11, 12, 13, 14, 15, 16, 17, 18, 22, 24, 25, 26, 27, 28, 29, 30, 31, 32, 33, 34, 38
	(kW)	–	5, 150, 125, 30, 75, 115, 190, 190, 275, 120, 180, 130, 155, 15, 35, 160, 335, 30, 20, 30, 110, 600, 275, 545, 85, 5, 15	–	90, 20, 215, 25, 75, 80, 165, 160, 125, 120, 130, 50, 25, 565, 505, 55, 125, 505, 60, 50, 30	–	115, 20, 115, 15, 60, 80, 80, 120, 200, 100, 105, 100, 150, 25, 130, 225, 30, 15, 30, 610, 560, 185, 390, 85, 395, 75	–	115, 20, 110, 15, 60, 80, 80, 120, 200, 102, 105, 100, 150, 25, 130, 225, 30, 15, 30, 610, 560, 185, 385, 85, 395, 75
BESS allocation	**Bus**	–	–	31	38	–	–	35	–
	(kW)	–	–	200	625	–	–	3000	–
	(kWh)	–	–	875	3500	–	–	5000	–
EV chargers allocation	**Bus**	–	–	–	–	29, 34, 35, 38	29, 34, 38	30, 35, 36, 38	29, 34, 38
	Number	–	–	–	–	55, 100, 30, 100	85, 100, 100	15, 100, 70, 100	85, 100, 100

5.6 Conclusions

This chapter presents a smart planning approach to accommodate PEV charging load in distribution networks. The presented approach can help the distribution companies and investors to optimize their investments. The planning method utilizes probabilistic approaches to optimally allocate PEV charging stations, PV units and BESS systems to maximize the profit of the system operators and investors. The proposed approach includes smart coordination of the PEV charging process, smart scheduling of the BESS units, and smart control of PV inverters. The planning problem is defined as MINLP, which is solved using, a combination between GA and deterministic optimization tool due to the problem complexity. Simulation results on a typical distribution system demonstrate that significant profit can be achieved by allocating PV units to support the PEV charging stations. On the other hand, the results proved that BESS units do not present significant support for PEV charging stations, either for commercial charging stations or residential charging stations. Although the results are entirely system dependent, the proposed method is generalizable and can be applied to any distribution network.

Chapter 6
Concluding remarks

6.1 Summary and Conclusions

The research in this thesis presents new approaches to optimally allocate PEV charging parking lots in conjunction with RES and BESS units in distribution networks under the smart grid paradigm.

The objective of the proposed planning aims to minimize the overall capital and operational costs. The operational costs include consideration of 1) coordinated PEV charging, 2) smart inverter control of renewable DG units, and 3) smart scheduling of BESS.

The research presented in this thesis is developed on three main stages presented in chapters 3, 4, and 5.

In chapter 3, an approach to optimally allocate RES DG is developed taking into consideration the uncertainty due to the intermittent nature of RES DG output power. The work also investigates the impacts of the technical constraints on the allocation process, to identify the most significant binding constraints. It is concluded in this chapter that constraints such as maximum number of DG units and maximum reverse power flow were found to be very significant to the results of the allocation process; however, beyond certain limit, the improvement is negligible.

In chapter 4, the developed approach in chapter 3 is extended to include consideration of BESS units. Chronological probabilistic models based on MCS are used in this work to encounter for the BESS characteristics. Simulation results on a typical distribution system demonstrate that significant profit can be achieved by allocating BESS units in addition to renewable DG units.

Chapter 5 presents a smart planning approach, which utilizes probabilistic approaches to optimally allocate PEV charging stations, PV units and BESS systems to maximize the profit of the system operators and investors. The proposed approach includes smart coordination of the PEV charging process, smart scheduling of the BESS units, and smart control of PV inverters. Due to the complexity of the proposed problem, it is split into two nested parts i.e. exterior and interior. The exterior and interior parts represent the installation and operation-scheduling problems respectively. Further, a combination between metaheuristic technique and deterministic technique has been utilized to manage exterior and interior parts concurrently.

Moreover, a new model for the PEV coordinated charging demand is introduced in this thesis, which is based on developing all possible scenarios during a calendar year of PEV arrivals and PEV requirements. Further, this model is converted to energy consumption model during the optimization process based on the optimal schedule of PEV charging and the technical limits of the distribution network. Simulation results on a typical distribution system demonstrate that significant profit can be achieved by allocating PV

units to support the PEV charging stations; on the other hand, the results proved that BESS units do not present significant support for PEV charging stations.

The main contribution of this thesis is the development of a new approach to allocate PEV smart charging stations in distribution networks in conjunction with RES and BESS. Moreover, as a by-product, a new probabilistic model for the PEV demand in smart grid is developed.

6.2 Directions for Future Work

In continuation of this research, the following subjects are suggested for future work:

- Investigating the benefits that can be offered by discharging of PEVs under the smart grids.
- Developing planning approaches to allocate PEV charging stations in microgrid systems.

Appendix A

The 123-bus test system load data

Table A.1 123-bus test system data [84]

Node	Load	Ph-1	Ph-1	Ph-2	Ph-2	Ph-3	Ph-4	Node	Load	Ph-1	Ph-1	Ph-2	Ph-2	Ph-3	Ph-4
	Mode	kW	kVAr	kW	kVAr	kW	kVAr		Mode	kW	kVAr	kW	kVAr	kW	kVAr
1	Y-PQ	40	20	0	0	0	0	**59**	Y-PQ	0	0	20	10	0	0
2	Y-PQ	0	0	20	10	0	0	**60**	Y-PQ	20	10	0	0	0	0
4	Y-PR	0	0	0	0	40	20	**62**	Y-Z	0	0	0	0	40	20
5	Y-I	0	0	0	0	20	10	**63**	Y-PQ	40	20	0	0	0	0
6	Y-Z	0	0	0	0	40	20	**64**	Y-I	0	0	75	35	0	0
7	Y-PQ	20	10	0	0	0	0	**65**	D-Z	35	25	35	25	70	50
9	Y-PQ	40	20	0	0	0	0	**66**	Y-PQ	0	0	0	0	75	35
10	Y-I	20	10	0	0	0	0	**68**	Y-PQ	20	10	0	0	0	0
11	Y-Z	40	20	0	0	0	0	**69**	Y-PQ	40	20	0	0	0	0
12	Y-PQ	0	0	20	10	0	0	**70**	Y-PQ	20	10	0	0	0	0
16	Y-PQ	0	0	0	0	40	20	**71**	Y-PQ	40	20	0	0	0	0
17	Y-PQ	0	0	0	0	20	10	**73**	Y-PQ	0	0	0	0	40	20
19	Y-PQ	40	20	0	0	0	0	**74**	Y-Z	0	0	0	0	40	20
20	Y-I	40	20	0	0	0	0	**75**	Y-PQ	0	0	0	0	40	20
22	Y-Z	0	0	40	20	0	0	**76**	D-I	105	80	70	50	70	50
24	Y-PQ	0	0	0	0	40	20	**77**	Y-PQ	0	0	40	20	0	0
28	Y-I	40	20	0	0	0	0	**79**	Y-Z	40	20	0	0	0	0
29	Y-Z	40	20	0	0	0	0	**80**	Y-PQ	0	0	40	20	0	0
30	Y-PQ	0	0	0	0	40	20	**82**	Y-PQ	40	20	0	0	0	0
31	Y-PQ	0	0	0	0	20	10	**83**	Y-PQ	0	0	0	0	20	10
32	Y-PQ	0	0	0	0	20	10	**84**	Y-PQ	0	0	0	0	20	10
33	Y-I	40	20	0	0	0	0	**85**	Y-PQ	0	0	0	0	40	20
34	Y-Z	0	0	0	0	40	20	**86**	Y-PQ	0	0	20	10	0	0
35	D-PQ	40	20	0	0	0	0	**87**	Y-PQ	0	0	40	20	0	0
37	Y-Z	40	20	0	0	0	0	**88**	Y-PQ	40	20	0	0	0	0
38	Y-I	0	0	20	10	0	0	**90**	Y-I	0	0	40	20	0	0
39	Y-PQ	0	0	20	10	0	0	**92**	Y-PQ	0	0	0	0	40	20
41	Y-PQ	0	0	0	0	20	10	**94**	Y-PQ	40	20	0	0	0	0
42	Y-PQ	20	10	0	0	0	0	**95**	Y-PQ	0	0	20	10	0	0
43	Y-Z	0	0	40	20	0	0	**96**	Y-PQ	0	0	20	10	0	0
45	Y-I	20	10	0	0	0	0	**98**	Y-PQ	40	20	0	0	0	0
46	Y-PQ	20	10	0	0	0	0	**99**	Y-PQ	0	0	40	20	0	0
47	Y-I	35	25	35	25	35	25	**100**	Y-Z	0	0	0	0	40	20
48	Y-Z	70	50	70	50	70	50	**102**	Y-PQ	0	0	0	0	20	10
49	Y-PQ	35	25	70	50	35	20	**103**	Y-PQ	0	0	0	0	40	20
50	Y-PQ	0	0	0	0	40	20	**104**	Y-PQ	0	0	0	0	40	20
51	Y-PQ	20	10	0	0	0	0	**106**	Y-PQ	0	0	40	20	0	0
52	Y-PQ	40	20	0	0	0	0	**107**	Y-PQ	0	0	40	20	0	0
53	Y-PQ	40	20	0	0	0	0	**109**	Y-PQ	40	20	0	0	0	0
55	Y-Z	20	10	0	0	0	0	**111**	Y-PQ	20	10	0	0	0	0
56	Y-PQ	0	0	20	10	0	0	**112**	Y-I	20	10	0	0	0	0
58	Y-I	0	0	20	10	0	0	**113**	Y-Z	40	20	0	0	0	0
								114	Y-PQ	20	10	0	0	0	0
								Total		760	410	375	225	520	285

Appendix B

The 38-bus test system data

Table B.2 38-bus test system data [86]

F	T	Ln	Line impedance in pu	To node - load	
				P	Q
1	2	1	0.000574+0.000293j	0.1	0.06
2	3	6	0.00307+0.001564j	0.09	0.04
3	4	11	0.002279+0.001161j	0.12	0.08
4	5	12	0.002373+0.001209j	0.06	0.03
5	6	13	0.0051+0.004402j	0.06	0.02
6	7	22	0.001166+0.003853j	0.2	0.1
7	8	23	0.00443+0.001464j	0.2	0.1
8	9	25	0.006413+0.004608j	0.06	0.02
9	10	27	0.006501+0.004608j	0.06	0.02
10	11	28	0.001224+0.000405j	0.045	0.03
11	12	29	0.002331+0.000771j	0.06	0.035
12	13	31	0.009141+0.007192j	0.06	0.035
13	14	32	0.003372+0.004439j	0.12	0.08
14	15	33	0.00368+0.003275j	0.06	0.01
15	16	34	0.004647+0.003394j	0.06	0.02
16	17	35	0.008026+0.010716j	0.06	0.02
17	18	36	0.004558+0.003574j	0.09	0.04
2	19	2	0.001021+0.000974j	0.09	0.04
19	20	3	0.009366+0.00844j	0.09	0.04
20	21	4	0.00255+0.002979j	0.09	0.04
21	22	5	0.004414+0.005836j	0.09	0.04
3	23	7	0.002809+0.00192j	0.09	0.05
23	24	8	0.005592+0.004415j	0.42	0.2
24	25	9	0.005579+0.004366j	0.42	0.2
6	26	14	0.001264+0.000644j	0.06	0.025
26	27	15	0.00177+0.000901j	0.06	0.025
27	28	16	0.006594+0.005814j	0.06	0.02
28	29	17	0.005007+0.004362j	0.12	0.07
29	30	18	0.00316+0.00161j	0.2	0.6
30	31	19	0.006067+0.005996j	0.15	0.07
31	32	20	0.001933+0.002253j	0.21	0.1
32	33	21	0.002123+0.003301j	0.06	0.04
8	34	24	0.012453+0.012453j	0	0
9	35	26	0.012453+0.012453j	0	0
12	36	30	0.012453+0.012453j	0	0
18	37	37	0.003113+0.003113j	0	0

Bibliography

[1] W. Su, H. Eichi, W. Zeng, and M.-Y. Chow, "A survey on the electrification of transportation in a smart grid environment," *IEEE Transactions on Industrial Informatics*, vol. 8, pp. 1-10, 2012.

[2] *International Energy Agency*. Available [Online]: http://www.iea.org, 2015

[3] W. Di, D. C. Aliprantis, and K. Gkritza, "Electric Energy and Power Consumption by Light-Duty Plug-In Electric Vehicles," *IEEE Transactions on Power Systems*, vol. 26, pp. 738-746, 2011.

[4] Q. Gong, S. Midlam-Mohler, V. Marano, and G. Rizzoni, "Study of PEV charging on residential distribution transformer life," *IEEE Transactions on Smart Grid*, vol. 1, pp. 404-412, 2012.

[5] S. Rezaee, E. Farjah, and B. Khorramdel, "Probabilistic analysis of plug-in electric vehicles impact on electrical grid through homes and parking lots," *IEEE Transactions on Sustainable Energy*, vol. 4, pp. 1024-1033, 2013.

[6] M. S. ElNozahy and M. M. Salama, "A comprehensive study of the impacts of PHEVs on residential distribution networks," *IEEE Transactions on Sustainable Energy*, vol. 5, pp. 332-342, 2014.

[7] A. Mohamed, V. Salehi, T. Ma, and O. Mohammed, "Real-time energy management algorithm for plug-in hybrid electric vehicle charging parks involving sustainable energy," *IEEE Transactions on Sustainable Energy*, vol. 5, pp. 577-586, 2014.

[8] U. C. Chukwu and S. M. Mahajan, "Real-time management of power systems with V2G facility for smart-grid applications," *IEEE Transactions on Sustainable Energy*, vol. 5, pp. 558-566, 2014.

[9] U. C. Chukwu and S. M. Mahajan, "V2G parking lot with pv rooftop for capacity enhancement of a distribution system," *IEEE Transactions on Sustainable Energy*, vol. 5, pp. 119-127, 2014.

[10] C. Wu, C. Chung, F. Wen, and D. Du, "Reliability/cost evaluation with PEV and wind generation system," *IEEE Transactions on Sustainable Energy*, vol. 5, pp. 273-281, 2014.

[11] M. Brenna, A. Dolara, F. Foiadelli, S. Leva, and M. Longo, "Urban scale photovoltaic charging stations for electric vehicles," *IEEE Transactions on Sustainable Energy*, vol. 5, pp. 1234-1241, 2014.

[12] S. F. Abdelsamad, W. G. Morsi, and T. S. Sidhu, "Impact of Wind-Based Distributed Generation on Electric Energy in Distribution Systems Embedded With Electric Vehicles," *IEEE Transactions on Sustainable Energy*, vol. 6, pp. 79-87, 2015.

[13] W. Kempton and J. Tomić, "Vehicle-to-grid power implementation: From stabilizing the grid to supporting large-scale renewable energy," *Journal of Power Sources*, vol. 144, pp. 280-294, 2005.

[14] S. Vazquez, S. M. Lukic, E. Galvan, L. G. Franquelo, and J. M. Carrasco,

"Energy storage systems for transport and grid applications," *IEEE Transactions on Industrial Electronics*, vol. 57, pp. 3881-3895, 2010.
[15] C. Hill, M. C. Such, D. Chen, J. Gonzalez, and W. M. Grady, "Battery energy storage for enabling integration of distributed solar power generation," *IEEE Transactions on Smart Grid*, vol. 3, pp. 850-857, 2012.
[16] M.-S. Lu, C.-L. Chang, W.-J. Lee, and L. Wang, "Combining the wind power generation system with energy storage equipments," in *Industry Applications Society Annual Meeting, 2008. IAS'08. IEEE*, 2008, pp. 1-6.
[17] C. Jin, J. Tang, and P. Ghosh, "Optimizing electric vehicle charging with energy storage in the electricity market," *IEEE Transactions on Smart Grid*, vol. 4, pp. 311-320, 2013.
[18] E. Wesoff, "Solar frontier CIS PV panels charging the Nissan Leaf," *Greentech Media*, 2011.
[19] N. Halverson, "Electric vehicle charger powered by wind and solar," *Discovery News*, 2011.
[20] R. Liu, L. Dow, and E. Liu, "A survey of PEV impacts on electric utilities," in *Innovative Smart Grid Technologies (ISGT), 2011 IEEE PES*, 2011, pp. 1-8.
[21] *Natural resources Canada*. Available: [online]http://www.nrcan.gc.ca/energy/ renewable-electricity/ 7295, 2015
[22] *Ontario's supply mix*. Independent Electricity System Operator. Available [online] : http://www.ieso.ca/Pages/Ontario%27s-Power-System/Supply-Mix/default.aspx, 2015
[23] G. M. Masters, *Renewable and efficient electric power systems*: John Wiley & Sons, 2013.
[24] Canadian Wind Energy Association. Available [online]: http://canwea.ca/wind-energy/ installed-capacity, 2015
[25] J. Hetzer, D. C. Yu, and K. Bhattarai, "An economic dispatch model incorporating wind power," *IEEE Transactions on Energy Conversion*, vol. 23, pp. 603-611, 2008.
[26] W. m. o. . *Guide to meterological instruments and methods of observation*: Secretariat of the World Meteorological Organization, 1996.
[27] M. F. Shaaban, Y. M. Atwa, and E. F. El-Saadany, "DG allocation for benefit maximization in distribution networks," *IEEE Transactions on Power Systems*, vol. 28, pp. 639-649, 2013.
[28] Y. M. Atwa, E. F. El-Saadany, M. M. A. Salama, and R. Seethapathy, "Optimal renewable resources mix for distribution system energy loss minimization," *IEEE Transactions on Power Systems*, vol. 25, pp. 360-370, 2010.
[29] S. H. Jangamshetti and V. G. Rau, "Site matching of wind turbine generators: a case study," *IEEE Transactions on Energy Conversion*, vol. 14, pp. 1537-1543, 1999.
[30] Technology Roadmap: Solar Photovoltaic Energy - 2014 edition. Available [online]: https://www.iea.org/publications/freepublications/publication/

technology-roadmap-solar-photovoltaic-energy---2014-edition.html, 2015
[31] Ontario Power Authority FIT/microFIT price schedule http://microfit.powerauthority.on.ca/sites/default/files/page/FIT%20Price%20Schedule%202014-09-30.pdf, 2015
[32] A. Awad, "Novel Planning and Market Models for Energy Storage Systems in Smart Grids," University of Waterloo, 2014.
[33] S. M. Schoenung and C. Burns, "Utility energy storage applications studies," *Energy Conversion, IEEE Transactions on*, vol. 11, pp. 658-665, 1996.
[34] I. Hadjipaschalis, A. Poullikkas, and V. Efthimiou, "Overview of current and future energy storage technologies for electric power applications," *Renewable and sustainable energy reviews*, vol. 13, pp. 1513-1522, 2009.
[35] S. Choi, K. Tseng, D. Vilathgamuwa, and T. Nguyen, "Energy storage systems in distributed generation schemes," in *Power and Energy Society General Meeting-Conversion and Delivery of Electrical Energy in the 21st Century, 2008 IEEE*, 2008, pp. 1-8.
[36] T. Sels, C. Dragu, T. Van Craenenbroeck, and R. Belmans, "Overview of new energy storage systems for an improved power quality and load managing on distribution level," in *Electricity Distribution, 2001. Part 1: Contributions. CIRED. 16th International Conference and Exhibition on (IEE Conf. Publ No. 482)*, 2001, p. 5 pp. vol. 4.
[37] R. B. Schainker, "Executive overview: energy storage options for a sustainable energy future," in *Power Engineering Society General Meeting, 2004. IEEE*, 2004, pp. 2309-2314.
[38] J. D. Boyes and N. H. Clark, "Technologies for energy storage. flywheels and super conducting magnetic energy storage," in *Power Engineering Society Summer Meeting, 2000. IEEE*, 2000, pp. 1548-1550.
[39] Toronto Hydro. Introducing the first urban community energy storage project, Available: http://www.torontohydro.com/sites/electricsystem/powerup/Pages/CommunityEnergyStorage.aspx, 2015
[40] Independent Electricity System Operator. Energy Storage Procurement – IESO. Available [online] http://www.ieso.ca/Pages/Participate/Energy-Storage-Procurement/ default.aspx, 2015
[41] MHC, "Energy Storage in Australia," report submitted to Clean Energy Council, Nov. 2012. Available [online] https://www.cleanenergycouncil.org.au/dam/cec/policy-and-advocacy/reports/2013/Energy-Storage-Study/Energy%20Storage%20Study.pdf, 2015
[42] B. C. Chan, "The state of the art of electric, hybrid, and fuel cell vehicles," *Proceedings of the IEEE*, vol. 95, pp. 704-718, 2007.
[43] M. F. Shaaban and E. F. El-Saadany, "Accommodating high penetrations of PEVs and renewable DG considering uncertainties in distribution systems," *IEEE Transactions on Power Systems*, vol. 29, pp. 259-270, 2014.
[44] V. Monteiro, H. Gonçalves, J. C. Ferreira, and J. L. Afonso, "Batteries charging

systems for electric and plug-in hybrid electric vehicles," 2012.
[45] F. Marra, G. Y. Yang, C. Traholt, E. Larsen, C. N. Rasmussen, and S. You, "Demand profile study of battery electric vehicle under different charging options," in *Power and Energy Society General Meeting, 2012 IEEE*, 2012, pp. 1-7.
[46] H. Khan and M. A. Choudhry, "Implementation of Distributed Generation (IDG) algorithm for performance enhancement of distribution feeder under extreme load growth," *International Journal of Electrical Power & Energy Systems,* vol. 32, pp. 985-997, 2010.
[47] M. Kashem, A. D. Le, M. Negnevitsky, and G. Ledwich, "Distributed generation for minimization of power losses in distribution systems," in *Power Engineering Society General Meeting, 2006. IEEE*, 2006, p. 8 pp.
[48] D. Q. Hung, N. Mithulananthan, and R. C. Bansal, "Analytical expressions for DG allocation in primary distribution networks," *IEEE Transactions on Energy Conversion,* vol. 25, pp. 814-820, 2010.
[49] A. A. Abou El-Ela, S. M. Allam, and M. M. Shatla, "Maximal optimal benefits of distributed generation using genetic algorithms," *Electric Power Systems Research,* vol. 80, pp. 869-877, 2010.
[50] W. El-Khattam, K. Bhattacharya, Y. Hegazy, and M. M. A. Salama, "Optimal investment planning for distributed generation in a competitive electricity market," *IEEE Transactions on Power Systems,* vol. 19, pp. 1674-1684, 2004.
[51] F. S. Abu-Mouti and M. E. El-Hawary, "Optimal distributed generation allocation and sizing in distribution systems via artificial bee colony algorithm," *IEEE Transactions on Power Delivery,* vol. 26, pp. 2090-2101, 2011.
[52] L. F. Ochoa, A. Padilha-Feltrin, and G. P. Harrison, "Evaluating distributed generation impacts with a multiobjective index," *IEEE Transactions on Power Delivery,* vol. 21, pp. 1452-1458, 2006.
[53] C. Wang and M. H. Nehrir, "Analytical approaches for optimal placement of distributed generation sources in power systems," *IEEE Transactions on Power Systems,* vol. 19, pp. 2068-2076, 2004.
[54] L. F. Ochoa and G. P. Harrison, "Minimizing energy losses: Optimal accommodation and smart operation of renewable distributed generation," *IEEE Transactions on Power Systems,* vol. 26, pp. 198-205, 2011.
[55] A. Alarcon-Rodriguez, E. Haesen, G. Ault, J. Driesen, and R. Belmans, "Multi-objective planning framework for stochastic and controllable distributed energy resources," *IET Renewable Power Generation,* vol. 3, pp. 227-238, 2009.
[56] L. F. Ochoa, A. Padilha-Feltrin, and G. P. Harrison, "Time-series-based maximization of distributed wind power generation integration," *IEEE Transactions on Energy Conversion,* vol. 23, pp. 968-974, 2008.
[57] Y. Zhao, Y. An, and Q. Ai, "Research on size and location of distributed generation with vulnerable node identification in the active distribution network," *IET Generation, Transmission & Distribution,* vol. 8, pp. 1801-1809, 2014.

[58] S. A. Arefifar and Y. A.-R. Mohamed, "DG mix, reactive sources and energy storage units for optimizing microgrid reliability and supply security," *IEEE Transactions on Smart Grid,* vol. 5, pp. 1835-1844, 2014.
[59] H. E. Farag, M. M. Abdelaziz, and E. El-Saadany, "Incorporating voltage regulator and load models in unbalanced power flow studies of active distribution systems," in *Power and Energy Society General Meeting, 2012 IEEE*, 2012, pp. 1-7.
[60] H. Lund, G. Salgi, B. Elmegaard, and A. N. Andersen, "Optimal operation strategies of compressed air energy storage (CAES) on electricity spot markets with fluctuating prices," *Applied thermal engineering,* vol. 29, pp. 799-806, 2009.
[61] J. Usaola, "Operation of concentrating solar power plants with storage in spot electricity markets," *IET renewable power generation,* vol. 6, pp. 59-66, 2012.
[62] J. Garcia-Gonzalez, D. la Muela, R. M. Ruiz, L. M. Santos, and A. M. González, "Stochastic joint optimization of wind generation and pumped-storage units in an electricity market," *IEEE Transactions on Power Systems,* vol. 23, pp. 460-468, 2008.
[63] A. S. Awad, T. H. EL-Fouly, and M. M. Salama, "Optimal ESS allocation and load shedding for improving distribution system reliability," *IEEE Transactions on Smart Grid*, vol. 5, pp. 2339-2349, 2014.
[64] Y. Zheng, Z. Y. Dong, F. J. Luo, K. Meng, J. Qiu, and K. P. Wong, "Optimal allocation of energy storage system for risk mitigation of DISCOs with high renewable penetrations," *IEEE Transactions on Power Systems*, vol. 29, pp. 212-220, 2014.
[65] W. Shuli, L. Hai, F. Qiang, D. C. Yu, and Z. Lijun, "Economic Allocation for Energy Storage System Considering Wind Power Distribution," *IEEE Transactions on Power Systems,* vol. 30, pp. 644-652, 2015.
[66] M. Nick, R. Cherkaoui, and M. Paolone, "Optimal allocation of dispersed energy storage systems in active distribution networks for energy balance and grid support," *IEEE Transactions on Power Systems,* vol. 29, pp. 2300-2310, 2014.
[67] Y. M. Atwa and E. El-Saadany, "Optimal allocation of ESS in distribution systems with a high penetration of wind energy," *IEEE Transactions on Power Systems,* vol. 25, pp. 1815-1822, 2010.
[68] A. S. A. Awad, T. H. M. El-Fouly, and M. M. A. Salama, "Optimal ESS Allocation for Load Management Application," *IEEE Transactions on Power Systems,* vol. 30, pp. 327-336, 2015.
[69] C. Siting, L. Hongyang, and K. Nahrstedt, "Charging facility planning for Electric Vehicles," in *Electric Vehicle Conference (IEVC), 2014 IEEE International*, 2014, pp. 1-7.
[70] Y. Ping, Z. Ting, L. Guangyu, J. Xiuchen, L. Guojie, S. Liangqi, *et al.*, "Energy scheduling and allocation in electric vehicle energy distribution networks," in *Innovative Smart Grid Technologies (ISGT), 2013 IEEE PES*, 2013, pp. 1-6.
[71] M. Eisel, J. Schmidt, and L. M. Kolbe, "Finding suitable locations for charging

stations," in *Electric Vehicle Conference (IEVC), 2014 IEEE International*, 2014, pp. 1-8.

[72] A. Dias, P. M. S. Carvalho, P. Almeida, and S. Rapoport, "Multi-objective distribution planning approach for optimal network investment with EV charging control," in *PowerTech, 2015 IEEE Eindhoven*, 2015, pp. 1-5.

[73] L. Chao, H. Yih-Fang, and V. Gupta, "A Consumer Behavior Based Approach to Multi-Stage EV Charging Station Placement," in *Vehicular Technology Conference (VTC Spring), 2015 IEEE 81st*, 2015, pp. 1-6.

[74] F. Baouche, R. Billot, R. Trigui, and N. E. El Faouzi, "Efficient Allocation of Electric Vehicles Charging Stations: Optimization Model and Application to a Dense Urban Network," *Intelligent Transportation Systems Magazine, IEEE*, vol. 6, pp. 33-43, 2014.

[75] M. H. Amini and A. Islam, "Allocation of electric vehicles' parking lots in distribution network," in *Innovative Smart Grid Technologies Conference (ISGT), 2014 IEEE PES*, 2014, pp. 1-5.

[76] S. Wagner, M. Götzinger, and D. Neumann, "Optimal location of charging stations in smart cities: A points of interest based approach," *Thirty Fourth International Conference on Information Systems*, Milan, 2013.

[77] M. Dogru, M. Andrews, J. Hobby, Y. Jin, and G. Tucci, "Modeling and optimization for electric vehicle charging infrastructure," in *24th annual POM conference Denver, Colorado, USA*, 2013.

[78] T. D. Chen, K. M. Kockelman, and M. Khan, "The electric vehicle charging station location problem: a parking-based assignment method for Seattle," in *Transportation Research Board 92nd Annual Meeting*, 2013, pp. 13-1254.

[79] F. He, D. Wu, Y. Yin, and Y. Guan, "Optimal deployment of public charging stations for plug-in hybrid electric vehicles," *Transportation Research Part B: Methodological*, vol. 47, pp. 87-101, 2013.

[80] E. Traut, C. Hendrickson, E. Klampfl, Y. Liu, and J. J. Michalek, "Optimal design and allocation of electrified vehicles and dedicated charging infrastructure for minimum life cycle greenhouse gas emissions and cost," *Energy Policy*, vol. 51, pp. 524-534, 2012.

[81] Y.-W. Wang and C.-C. Lin, "Locating road-vehicle refueling stations," *Transportation Research Part E: Logistics and Transportation Review*, vol. 45, pp. 821-829, 2009.

[82] Z. M. Salameh, B. S. Borowy, and A. R. A. Amin, "Photovoltaic module-site matching based on the capacity factors," *IEEE Trans. on Energy Conversion*, vol. 10, pp. 326-332, 1995.

[83] C. Singh and Y. Kim, "An efficient technique for reliability analysis of power systems including time dependent sources," *IEEE Trans. on Power Systems*, vol. 3, pp. 1090-1096, 1988.

[84] IEEE 123 Node Test Feeder [0nline]. Available: http://ewh.ieee.org/soc/pes/dsacom/testfeeders/, 2015

[85] P. M. Subcommittee, "IEEE reliability test system," *IEEE Transactions on Power Apparatus and Systems*, pp. 2047-2054, 1979.

[86] D. Singh and R. K. Misra, "Effect of load models in distributed generation planning," *IEEE Trans. on Power Systems*, vol. 22, pp. 2204-2212, 2007.

[87] C.-H. Lin, W.-L. Hsieh, C.-S. Chen, C.-T. Hsu, and T.-T. Ku, "Optimization of photovoltaic penetration in distribution systems considering annual duration curve of solar irradiation," *IEEE Trans. on Power Systems*, vol. 27, pp. 1090-1097, 2012.